MIXING CHARACTERISTICS IN DENSE-PHASE FLUIDIZED BED SYSTEMS

BY

MAHFUZUR RAHMAN KHAN

DEPARTMENT OF CHEMICAL ENGINEERING

INDIAN INSTITUTE OF TECHNOLOGY KANPUR

1969

MIXING CHARACTERISTICS IN DENSE-PHASE FLUIDIZED BED SYSTEMS

A Thesis Submitted
In Partial Fulfilment of the Requirements
for the Degree of

MASTER OF TECHNOLOGY

BY

MAHFUZUR RAHMAN KHAN

to the

DEPARTMENT OF CHEMICAL ENGINEERING

INDIAN INSTITUTE OF TECHNOLOGY KANPUR

1969

TO MY FATHER AND MOTHER

C E R T I F I C A T E

Certified that this work on "Mixing Characteristics in Dense-Phase Fluidized Bed Systems" has been carried out under my supervision and has not been submitted elsewhere for a degree.

A. Vasudev,
Ph.D. (Washington)
Assistant Professor of
Chemical Engineering
Indian Institute of Technology
Kanpur, U.P., India

ACKNOWLEDGEMENT

The author feels deeply indebted to Dr. A. Vasudev for his constant help, invaluable advice and illuminating guidance during the course of this investigation.

The author also wishes to acknowledge the assistance rendered by the technical staff of the Chemical Engineering Department and the Central Workshop in the fabrication of the experimental set-up.

Lastly, the author extends his sincere thanks to the Computer Centre for allotting sufficient computer time and to Mr. B.S. Pandey for typing the manuscript.

Author

ABSTRACT

This study concerns radial diffusion in the dense-phase particulately fluidized beds of cylindrical particles. Experiments were performed with a tracer dye diffusing from a point source into beds of insulation beads (size: 5.5 mm x 3.5 mm) fluidized in water.

In all, four sampling probes were used and samplings done at eight radial positions of the sampling probe. Concentration profiles were studied for 150,250,350 and 450 gm,weights of beds at a flow rate of 8 litres per minute. Concentration profiles were also studied for the 450 gm bed in the flow rate range of 6 to 13 liters per minute.

The experimental range of modified Reynolds number was from 173 to 374 encompassing fractions void between 0.56 and 0.70. Computations were made of eddy diffusivity and modified Peclet group. The diffusion model was based on a modified form of Fick's Law, solved for two different boundary conditions.

Results showed non-dependence of eddy diffusivity on radial positions and also a significant change in eddy diffusivity in transition from a fixed bed to the fluidized bed. Plots of modified Peclet group with modified Reynolds number indicated a peak in transition from the fixed state to the fluidized state of the bed signifying minimum mixing at the minimum fluidization point.

* * * *

CONTENTS

***

LIST OF TABLES

.....

LIST OF FIGURES

....

NOMENCLATURE

a	=	Fluid bed radius, cm.
AF	=	Actual flow rate, liter/min.
C	=	Concentration of diffusing material, gm/liter
C_A	=	Mixed average concentration in column effluent, gm/lit.
D_p	=	Particle diameter, cm.
D_L, E, E_1, E_2	=	Eddy diffusion coefficient, $Cm^2/sec.$
D_T	=	Tube diameter, cm.
F	=	Flow rate as shown by rotameter, liter/min.
H, H_1, H_2	=	Bed height, cm.
$J_o(\quad)$	=	Bessel function of first kind, zero order
LPM	=	Liter per minute
$N_{Pe}, N_{Pe_1}, N_{Pe_2}$	=	Modified Peclet number
N_{Re}	=	Modified Reynolds number.
PD	=	Pressure drop in fluid, gmf/cm^2
r	=	Radial distance, cm.
Rm	=	Pressure difference shown by monometer filled with CCl_4, cm.
t	=	Time, sec.
U	=	Average fluid velocity, cm/sec.
Z	=	Distance in the direction of flow, cm.
$\epsilon, \epsilon_1, \epsilon_2$	=	Fractions void
$(\beta_n a)$	=	Positive roots of Bessel function of first kind first order. Dividing roots by 'a' gives values of β_n.

INTRODUCTION

Fluidized systems have been of great interest in industry for the past two decades and have come into prominence for use as chemical reactors. In most cases the yields of such reactors are highest when the radial mass transfer processes are maximized and the axial mass transfer processes minimized. The complicated hydrodynamic situation in fluidization defies theoretical analysis, except for very simplified and inexact approaches. Consequently there has been increased effort in the direction of definitive experimentation.

The term "fluidization" was invented to describe a certain mode of contacting granular solids with fluids. The so-called fluidized bed results when a fluid is caused to flow upward through a bed of suitably sized solid particles at a velocity sufficiently high to buoy the particles and to impart to them a violently turbulent, fluid like motion. Fluid velocities must be used which are intermediate between the velocity which will just buoy the particle bed and the velocity which will sweep the bed out of its container. In other words, the fluidized bed is a relatively stable condition of fluid-solid contacting which is intermediate to a packed column, on one hand, and pneumatic transport on the other.

The behavior of a fluidized bed varies with the conditions of fluidization. If a fluid (say, water) is passed upward through a bed of solid particles, the fluid will flow through the interstices between the particles and a pressure loss will be realized. If the fluid flow rate is increased slowly, the pressure loss will increase slowly and eventually a point will be reached where the upward drag exerted on the particles by the fluid just equals the weight of the particles. At this point the bed is weightless. Increasing fluid velocity slightly will cause the pressure loss and hence the upward drag on the particles to increase, thereby exceeding the pull of gravity on the particles. The ascending fluid will therefore lift the particles, increasing the bed voidage and decreasing the interstitial velocity until the forces on the particles are again in balance. Further increases in fluid velocity will cause further bed expansion. Eventually the bed will expand beyond the limits of the containing vessel and the particles will be transported by the fluid stream. This type of behavior has been termed "particulate fluidization".

Originally the particles formed a so-called "fixed bed", the characteristics of which are that the particles contained in the bed are motionless and are supported by contact with each other.

There exists a certain rate of fluid flow at which the solids bed will be expanded to such point that the particles may move within the bed. This condition is known as "onset of

fluidization", or the "fluidizing point". A bed which has passed the fluidizing point is known as "a dense-phase fluidized bed", or simply as a "fluidized bed".

When the fluid velocity is only slightly above that required for the onset of fluidization, there results what is known as a "quiescent fluidized bed". In this state, which is also known as the "minimum-fluidization state", the particles in the bed display little or no mixing.

As the fluid velocity is somewhat increased, the bed expands and the solids tend to mix readily. This state is known as a "turbulent fluidized bed". If the fluid velocity is considerably increased, the bed expands greatly and a condition of great solids dilution is created. The solids are then entrained in the fluid and are carried upward. This state is known as "dilute fluidized phase".

The basic characteristics of the dense-phase fluidized bed are (1) a comparatively low bed voidage of the order of magnitude of, say, 50 to 70 per cent and (2) the fact that the solids bed as a whole is fixed relative to the wall of the confining vessel.

Particulate (Homogeneous) fluidization occurs in cases where the fluid and solid densities are not too different, where the particles are small, and therefore where the velocity of flow is low. The bed fluidizes evenly with each particle moving

individually through a relatively uniform mean free path. The solid phase has many of the characteristics of a gas. Particulate fluidization is achieved in high-density fluids with small density difference between particle and fluid, as in glass beads suspended in a rising stream of water.

Aggregative (non-homogeneous) fluidization occurs where the fluid and solid densities are greatly different or the particles are large. The velocity of flow will be relatively high. In this case, fluidization is uneven, and the fluid passes through the bed mainly in large bubbles. These bubbles burst at the surface spraying solid particles above the bed. Here, the bed has many of the characteristics of a liquid with the fluid acting as a gas bubbling through it. Experimentally, aggregative fluidization occurs with a gas as the fluid phase.

Intensive mixing of the solid material and fluid can occur in fluidized beds. Mixing assists some processes & hinders others; it has very important effects on heat and mass transfer and on chemical reactions. The study of mixing is therefore of considerabl practical interest and has occupied the attention of many researchers but because of its complexity the subject has still only been superficially investigated.

Mixing of the material in a fluidized bed permits equalization of the bed temperatures even when it is used for carrying out a process in which a large heat effect is involved; it also

leads to an increase in the heat transfer rate between a fluidized bed and heated or cooled walls surrounding it. Thus the temperature of the fluidized bed can be kept at a constant level.

Major application of fluidization goes to chemical conversion or synthesis. The maintenance of a uniform temperature is essential in controlling the selectivity of the desirable product and to eliminate or to reduce the amount of undesirable by-products resulting from side reactions. Along with the transfer of heat, the transfer of mass, especially its rate, becomes important in determining the rate of conversion in a fluidized reactor. For the design of a fluidized reactor it is necessary to have a quantitative knowledge of heat and mass transfer in such reactor.

The function of most solids used in fluidized systems is to act as a catalyst for some type of chemical reaction. In order for the solid particles to perform as catalysts, there must be intimate contact between the solids and reactant materials. Thus, in addition to a high level of heat transfer, this requires that mass be transferred from the bulk fluid to the catalyst surface and subsequently that the products of the reaction be transferred from the catalyst surface back into the bulk stream.

The mechanism of fluid mixing in fluidized beds is far from being satisfactorily understood. Although for the point of incipient fluidization, and slightly beyond, the fluid flow pattern is probably similar to that in fixed beds, the fact is

not of very much worth because the fixed-bed flow mechanism is itself still largely enigmatic. Fluid-mixing studies that have so far been reported for the dense-phase fluidized state are of a limited nature so far as equipment size, materials, and operating conditions are concerned [5]. Moreover, all studies were made in nonreactive systems.

Mixing of gases in fluidized beds has been the subject of a large number of investigations [6,7,8,9,10,17].

The importance of the present work lies in the fact that fluid mixing has been studied in a dense-phase particulately fluidized bed of uniform solid, nonspherical particles in water. The few investigations hitherto made in the liquid solid systems consist mainly in the study of fluid mixing in a bed of spherical particles fluidized in water. A review of these will be made in the following chapter.

Another important point worth mentioning is that the catalysts generally used in the fluidized bed reactors are not spherical but are more or less cylindrical in shape.

***

A REVIEW OF EARLIER INVESTIGATIONS

Wicke and Trawinski [1], Hanratty, Latinen and Wilhelm [2], Blickle and Kaldi [3] and Cairns and Prausnitz [4] have investigated fluid mixing in particulately fluidized beds of solid spherical particles.

Wicke and Trawinski [1] fluidized beds of glass spheres and alumina and plastic granules extending over a range of 0.9 to 12 mm diameter with water in tubes of 90 mm diameter. Tracer liquid (3N hydrochloric acid solution or hot water) was fed in continuously through a tube of 4- or 6-mm diameter placed axially with its outlet in the plane of the bed support screen. The concentrations of hydrochloric acid at various points were determined by electroconductivity probes. In those cases where hot water was used as tracer liquid, thermocouples were used as probes. The experimental data agreed approximately with the Gaussian distribution function:

$$C(r,\ Z) = k\,\frac{U}{Z}\,e^{-Ur^2/4D_L Z} \qquad (2.1)$$

where D_L is the liquid diffusivity, and k is a constant. Equation (2.1) resulted from an assumption that the distribution of the tracer into the main liquid proceeded according to the differential equation

$$\frac{\partial C}{\partial Z} = \frac{D_L}{U} \frac{\partial^2 C}{\partial r^2} \qquad (2.2)$$

which describes one-dimensional diffusion.

The diffusion coefficient, D_L, was found to depend on system variables as follows:

1. D_L increases linearly with the liquid flow rate.
2. D_L increases with particle diameter.

The above observations yield

$$D_L = 0.33\ UD_p^{0.85} \qquad (2.3)$$

The bases of the units of equation (2.3) are feet and hours. Fluidized-bed height and height above tracer injection had little or no effect on D_L, nor was the effect of solid material definitely established. There was good agreement between D_L values obtained from the acid injection and hot-water injection methods.

Hanratty, Latinen and Wilhelm [2] investigated the mixing of the fluid stream in a water-fluidized bed of glass spheres (D_p = 3 mm) in a 54-mm-diameter tube. A tracer (aqueous solution of methylene blue dye) was fed in axially through a tracer injection tube of 1/8 in. O.D. and 1/16 in. I.D. Liquid samples were taken at various points in the bed and analyzed electrophotometrically. This investigation covered a much wider range of bed expansions than that of Wicke and Trawinski. The Hanratty et.al. paper goes extensively into a theoretical discussion of

turbulence, and it is pointed out that, in a particulately fluidizing bed operating between extreme voidages ranging from fixed bed to the empty tube, the mixing properties may be defined by the Peclet number, a turbulence intensity, a measure of the lifetime of a turbulent eddy, and a so-called turbulence scale. A plot of the Peclet number, $D_p U/D_L$ versus the Reynolds number produced, for a particulately fluidizing bed, a curve that passes through a minimum. This occurs at a fluid mass velocity for which the bed has a voidage of about 70 per cent.

For cross sections that were substantially above the dye injection point the dye distribution was found to be Gaussian. For lateral positions closer to the origin of the dye the experimental distribution data deviated from the Gauss curve in the extreme radial regions. The distribution data seemed to be of the type reported by Wicke and Trawinski.

Blickle and Kaldi [3] used a noncontinuous tracer feed (NaCl solution) and determined the change in concentration at the bed outlet. The mixing coefficient increased initially with increase in the superficial fluid velocity but then began to fall off. The authors explained that one reason for this could be the marked decrease in particle concentration in the bed at large fluid velocities.

Cairns and Prausnitz [4] studied the longitudinal mixing of water in fluidized beds of glass (D_p = 3.2 mm) and lead (D_p = 113 and 3.0 mm) spheres in 50-and 100-mm-diameter along the

axis at intervals of five bed diameters from the electrolyte tracer feed point. The electrolyte (sodium nitrate solution) was introduced simultaneously at 156 points over the cross section; even at an axial distance of five particle diameters the nonuniformity of the concentration profile did not exceed 9 per cent when the electrolyte was supplied continuously. By using a by-pass line with a rapid-acting solenoid reversing valve it was possible to cut off the electrolyte supply very rapidly. Radial profiles of the electrical conductivity were obtained by using small 3-mm-diameter probes to measure the electrical conductivity of a volume of the order of 1 mm. The electrolyte concentration was assumed proportional to the electrical conductivity. The bed voidage had an important effect on the intensity of longitudinal mixing; maximum mixing was observed at a bed voidage of 70 per cent. The effective longitudinal turbulent diffusivity depended directly on the bulk density of the particles and the ratio of bed diameter to particle diameter, D_T/D_p. The turbulent diffusivity is a function of the product of a characteristic length and a characteristic velocity; a nonuniform profile of the longitudinal diffusivity. According to the data of Cairns and Prausnitz, the ratio of the mean-longitudinal turbulent diffusivity to the radial diffusivity was 20-30 under conditions of maximum nonuniformity of the fluid velocity profile of $\pm$20 per cent.

EQUIPMENT, PROCEDURE AND EXPERIMENTAL DETAILS

Particle Specifications:

The particulately fluidized bed used in the present work consisted of uniformly sized cylindrical insulation beads suspended in an upward stream of water flowing in a 57-mm tube. The equivalent diameter of the bead was 4.65mm. The actual density of the particle was 2.44 GM/CC. The bed density of the particles was 1.07 GM/CC.

Apparatus:

A sketch of the equipment used is shown in Figure 3.1. Features of the design are as follows:

The main test column was a brass tube 5.7 cm.I.D., 38.1 cm. long. Aqueous methylene blue dye solution of concentration 2GM/1,000 ml. was admitted to the fluidized bed of particles from a centrally located copper tube entering from the bottom. The tracer tube was 1/16 in.I.D., 1/8 in.O.D., and its point of injection was kept at a position flush with the support plate. The tracer injection system consisted of a Beckmann solution metering pump (a piston and cylinder arrangement) which received the dye from an overhead storage tank. The pump worked at 115 volts and had a range of delivering 0-20 ml./min. The circular scale on the pump indicated the flow being delivered

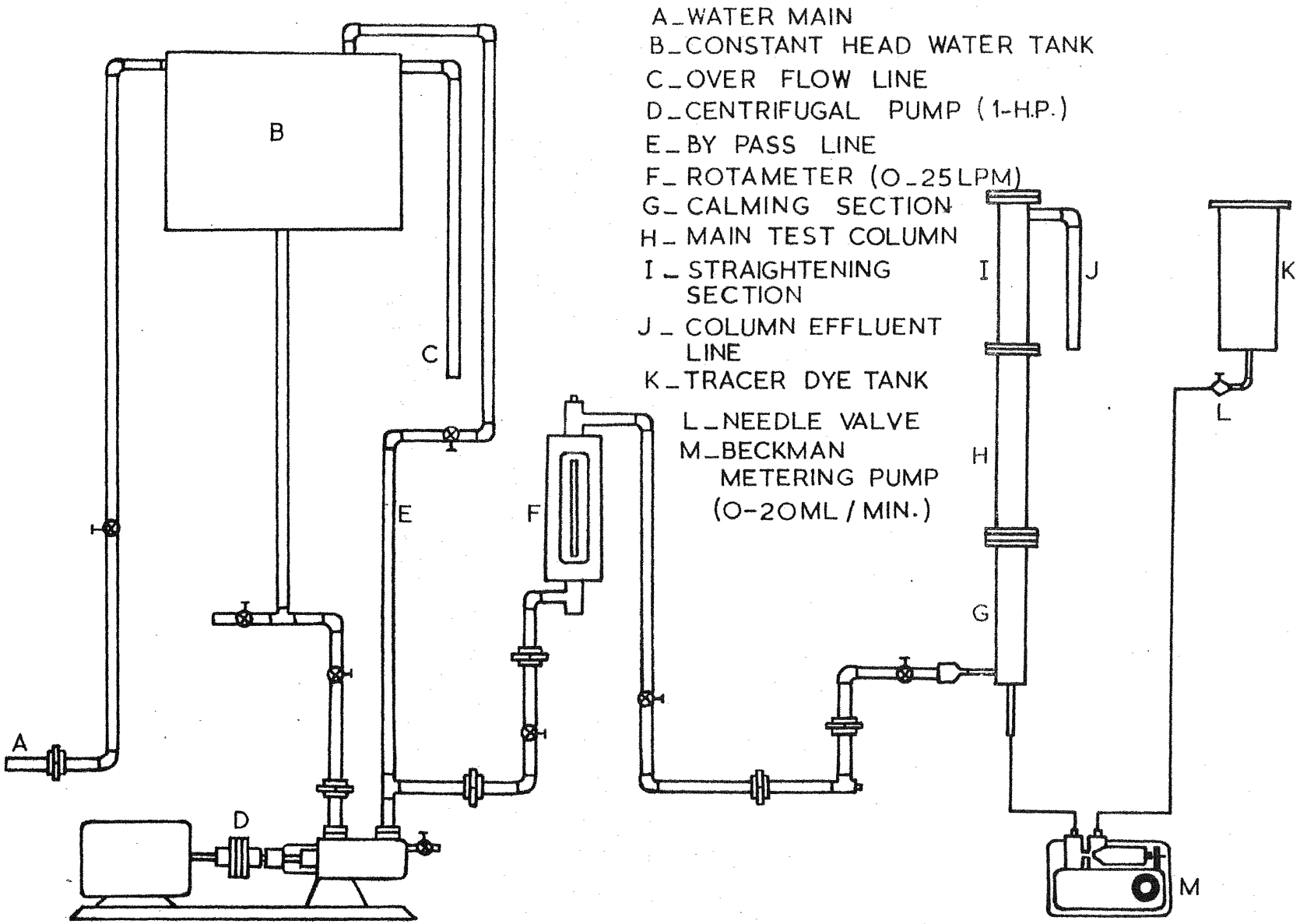

FIG.3.1_EQUIPMENT ARRANGEMENT FOR DIFFUSION STUDIES IN FLUIDIZED BEDS

in ml./min. The scale was calibrated so that an accurately known volume of liquid was being delivered per unit of time.

A calming section preceded the main test column to ensure a uniform-flow profile and to break up any large-scale eddies which might have formed. The calming section consisted of a 12 in. length of Brass piping packed with 1/4 in.glass spheres.

A straightening section made of glass tube 5.7 cm.I.D. and 12 in. long was provided on the top of the main test column. This section helped in minimizing the end effect at the exist of main test section and checking the entrainment of air bubbles, if any, in the column stream.

The main water stream was pumped to the bottom of the calming section by means of a 1 hp. centrifugal pump.

The support plate for the bed was a 5/16 in. thick perforated distributor plate with uniform 1/32 in. holes. The holes were arranged so that the open area was about 38 per cent of the area of the test section. The flow distributor ensured that flow entering the test section possessed a relatively flat velocity profile.

Water flow rates were measured by means of a rotameter having a range of 0-25 liter/min., and the tracer-dye flow rate was determined from the known water flow rate and the average concentration in the column effluent.

The sampling probe mechanism is shown in Figure 3.2. The sampling probe traversed radially. It consisted of a horizontal section of 1/16 in. I.D. and 1/8 in. O.D. Copper tubing bent into a vertical segment at its sampling point. The probe mechanism consisted of a cylindrical piece of brass 1 in. O.D., 7/8 in. I.D. and 3 in. long. It was threaded inside with one end open and the other closed except for a central hole of 1/8 in. diameter. Another cylindrical piece of brass 7/8 in. diameter and 3 in. long could be fitted into the piece mentioned above by means of threads (24 thread/in.) on its outside. There was a coaxial hole 1/8 inch diameter drilled throughout the piece. The sampling tube was pushed through this hole and was made to have a tight fit so that whenever the inner cylindrical piece of brass was rotated the sampling tube also rotated alongwith. The probe mechanism was fitted by means of threads into a socket brazed on the surface of the test column so that the sampling tube with its vertical segment entered the test column through a hole (slightly bigger than the O.D. of the tube) drilled through the surface of the column. The position of the tip of the sampling tube was so adjusted that it could be moved radially from the axis of the test column to a position near the wall of the column. The radial position of the sampling tip of the probe at any time could be read from a horizontal scale fixed onto the probe mechanism. In all there were used five sampling probes alongwith their mechanisms fitted at intervals of $1\frac{1}{2}$ in. on the column starting from the bottom.

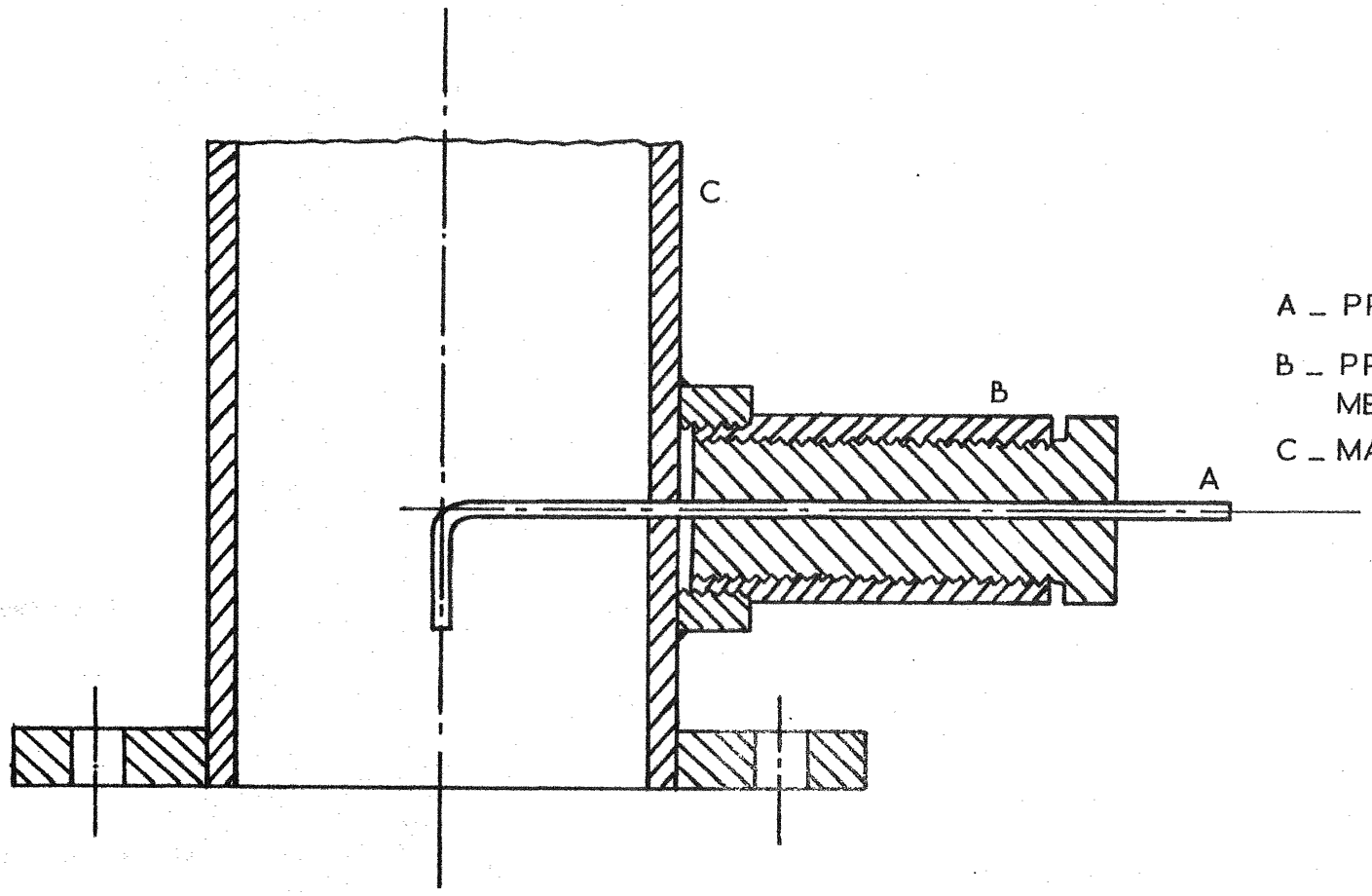

A _ PROBE.

B _ PROBE MOVEMENT MECHANISM

C _ MAIN TEST COLUMN

NOTE _ SECTIONAL SKETCH, NOT TO SCALE

FIG. 3.2 _ PROBE MECHANISM

Probe samples were analyzed with a spectronic-20 calorimeter at a wavelength of 594 mμ. The colorimeter was first calibrated for the tracer-dye by noting the Transmittance of a solution of known concentration.

In order to facilitate a visual study of the bed expansions versus the flow rates a glass column exactly identical with the brass-made main test column was procured. The glass column was fitted into the place of the main test column and all visual studies of bed expansions for different flow rates and different bed weights were carried out.

Procedure:

Data was obtained over a range of fluidized bed properties depending on the flow rates, bed heights and fractions void.

The operating procedure was as follows. After the lines were flushed, water was admitted to the column which contained a known weight of beads. The flow rate was maintained at a predetermined value. After an initial flushing of lines, the dye rate was adjusted to a velocity slightly less than that of the surrounding water stream. Time-average tracer samples were secured by a slow, uniform withdrawl over a period ranging from 2 to 3 minutes. Sample compositions do not depend on withdrawl rates at these low withdrawl velocities.

Rotameter Calibration:

The rotameter had a range of 0-25 LPM. Its calibration was done by noting the volume of water flowing in a known time. This volume expressed in terms of litre per minute was plotted against the reading indicated by the rotameter. Similar points were collected by increasing and decreasing the flow rates. A set of points was thus obtained. A line was drawn through them which passed through the origin. The calibration data are shown in Table 5.1 and the plot is shown in Fig. 5.1.

Pressure Drop Data:

Pressure drop measurements were made by means of a manometer filled with CCl_4 colored with iodine. Pressure taps were provided in the test column. Pressure drop data were collected for various flow rates starting from the lowest rotameter reading. The data are shown in Table 5.2. Figure 5.2 shows a plot of log (pressure drop in fluid) versus log (fluid velocity). This curve is characteristic of the fluidized bed under study.

Void Fraction Data:

To find the void fraction of the solids bed at any height it is essential to have a known fraction void at a known height. The void fraction at any other height can then be calculated by the following equation:

$$H_2/H_1 = (1- \epsilon_1)/(1- \epsilon_2) \qquad (3.1)$$

The initial bed heights and the corresponding fractions void were

as follows:

150 gm bed : H = 5.4 cm., ϵ = 0.56

250 gm bed : H = 9.0 cm., ϵ = 0.56

350 gm bed : H =12.6 cm., ϵ = 0.56

450 gm bed : H =16.3 cm., ϵ = 0.56

Sampling-Probe Placements:

In all, four sampling probes were used. The longitudinal placements of the probes measured from the support plate were as follows:

Probe No.1 - Z = 2.475 cm.

Probe No.2 - Z = 6.285 cm.

Probe No.3 - Z = 10.095 cm.

Probe No.4 - Z = 13.905 cm.

Radial Positions of the Sampling-Probe:

The sampling probe was displaced radially from the axis of the column towards the wall by steps corresponding to two rotations of the Knurled head of the probe mechanism. Since there are 24 threads per inch on the rotating cylinder of the probe mechanism the sampling tip of the probe will be displaced by steps of 0.2117 cm. along the radius of the column. Technically speaking there were nine radial positions of the probe available which are as follows:

Radial position No.1 - r = 0.0 cm.

Radial position No.2 - r = 0.2117 cm.

Radial position No.3 - r = 0.423 cm.

Radial position No.3 - r = 0.635 cm.

Radial position No.5 - r = 0.846 cm.

Radial position No.6 - r = 1.058 cm.

Radial position No.7 - r = 1.27 cm.

Radial position No.8 - r = 1.481 cm.

Radial position No.9 - r = 1.692 cm.

Spectronic-20 Colorimeter:

In order to use the Spectronic-20 Colorimeter for the colorimetric analysis of the probe samples, the particular wavelength was found at which the tracer solution (aqueous solution of methylene blue dye) indicated maximum absorbance on the scale. The wavelength was found to be 594mμ. All the probe samples were analyzed at this wavelength.

Colorimeter Calibration:

The colorimeter mentioned above indicates the strength of a solution in terms of Transmittance. So a calibration of the colorimeter is necessary in terms of concentration versus transmittance.

A. Relationship of Transmittance and Concentration:

The Transmittance (T) of a colored solution, when examined with monochromatic light having the same wavelength as the characteristic absorption band of the considered constituent, generally bears a simple mathematical relationship to the concentration, "C", and Transmittance, "T", may be expressed by a simple formula, provided certain requirements are fully met. These requirements are:

1. The "T" measurement must be made with monochromatic light.
2. The "T" measurement must be made at a wavelength where the characteristic absorption of the constituent is at a maximum, or where the change in absorption with changes in wavelength is small.
3. The Reference must be so selected that the concentration "C" equals zero when "T" = 100%
4. The nature of the sample solution must be such that Transmittance "T" responds only to changes in "C" of the desired constituent.

B. Lambert-Beer Law. C-T Calibration Curve:

The expression which relates concentration "C" to Transmittance "T", under these conditions, is known as the Lambert-Beer Law and may be written as follows:

$$C = - K \log T \qquad (3.2)$$

This equation significantly states that any concentration, C, of a given solution is proportional to the log of its corresponding transmittance, T. This means that the Concentration-Transmittance (C-T) graph of this relationship will be a straight line if plotted on semi-log coordinates, and such a C-T graph obviously constitutes a calibration by which the concentration corresponding to any particular T value may be determined.

The equation further states that this specified straight line will always intersect the point (C=0, T = 100%). Accordingly

it is possible to prepare the C-T calibration graph of an analytical method without calculations:

The T of one solution of known concentration C is simply determined. This known point is plotted on semi-log coordinates and then a straight line is drawn intersecting this point and the point (C = 0, T = 100%). This line is the C-T calibration graph of the method.

The aqueous solution of methylene blue dye that was accurately prepared to determine the "Known point" had a concentration C = 0.01 gm/litre. Its transmittance was found by means of the colorimeter to be T = 14.5%.

In order to achieve high accuracy in analyzing the probe samples, no calibration graph was drawn. Instead, a computer program was written for the equation (3.2) along with the two known points (C = 0.01, T = 14.5) and (C = 0, T = 100). All the transmittance data for the probe samples were fed along with this program. The program is shown in Appendix-I.

Analysis of Probe Samples:

Samples of liquid containing the tracer were drawn from the solids bed by the radial displacement of the sampling probe. To start with, the first sample was collected at r=0.0, i.e., at the axis of the column. The second sample was collected at r = 0.2117 cm. The third sample was collected at the third radial position and so on. During the collection of the above mentioned samples, a sample was also collected of the mixed effluent from

the column going to the drain. The samples were analyzed by means of the colorimeter and their transmittances, T's, were noted. The transmittance T_A of the sample of the mixed effluent was also noted. The C's corresponding to the T's and C_A corresponding to the T_A were found by computation with the help of the program in Appendix-I.

***

DEVELOPMENT OF THE MASS TRANSFER MODEL

The Mass Transfer Model for the system under study will follow the model developed for homogeneous isotropic systems involving turbulent diffusion by Hanratty, Latinen and Wilhelm [2].

Systems involving molecular diffusion may be described by the Fick's Law differential equation using appropriate boundary conditions:

$$\frac{\partial C}{\partial t} = \nabla\cdot(D\,\nabla C) \qquad (4.1)$$

The use of this equation implicitly involves the assumption that the diffusion characteristics of particles contained in a differential volume are independent of their previous history, i.e., the length of time they have been in the field. In turbulent diffusion, however, no such independence is encountered, i.e., D is a function of time. Fick's Law, therefore, may not be used to describe the diffusion of particles which have been in the field for different lengths of time.

It has been shown that equation (4.1) with a diffusion coefficient which varies with time can be used to describe the behavior of a single instantaneous source or sink of mass

$$\frac{\partial C}{\partial t} = \phi(t)\ \nabla^2 C \qquad (4.2)$$

For a cylindrical polar-coordinate system with radial symmetry equation (4.2) assumes the following forms for the case in which the diffusion in the Z direction is important and also for the case in which it is negligible:

$$\frac{\partial C}{\partial t} = \phi(t)\left[\frac{\partial^2 C}{\partial r^2} + \frac{1}{r}\ \frac{\partial C}{\partial r} + \frac{\partial^2 C}{\partial Z^2}\right] \qquad (4.3)$$

$$\frac{\partial C}{\partial t} = \phi(t)\left[\frac{\partial^2 C}{\partial r^2} + \frac{1}{r}\ \frac{\partial C}{\partial r}\right] \qquad (4.4)$$

If N units of material, or N units per unit length for the two-dimensional case, emitted into the field at zero time from a position r=0, Z=0, are considered, the solutions of equations (4.3) and (4.4) for boundary conditions

$$t > 0$$

$$C \longrightarrow 0, \text{ as } r \longrightarrow \infty;$$

$$C \longrightarrow 0, \text{ as } Z \longrightarrow \infty;$$

are respectively

a) longitudinal diffusion important:

$$C = \frac{N}{(2\pi)^{3/2}\left[\int_0^t 2\phi\,dt\right]^{3/2}} \cdot \exp\left[-\frac{r^2 + Z^2}{2\int_0^t 2\phi\,dt}\right] \qquad (4.5)$$

b) negligible longitudinal diffusion:

$$C = \frac{N}{(2\pi)\left[\int_0^t 2\phi\,dt\right]} \cdot \exp\left[-\frac{r^2}{2\int_0^t 2\phi\,dt}\right] \qquad (4.6)$$

When the diffusing time is long enough so that the material reaches the container walls, the boundary conditions become for $t > o$

$$Z = +\infty , \quad C = C_A ;$$

$$Z = -\infty , \quad C = 0 ;$$

$$r = a , \quad \frac{\partial C}{\partial r} = 0 ; \quad a = \text{column radius}$$

The solutions of equations (4.3) and (4.4) are then

c) longitudinal diffusion important

$$C = \frac{N \exp\left\{-\frac{Z^2}{4\int_o^t \phi\, dt}\right\}}{\pi a^2 \sqrt{2\pi}\left[\int_o^t 2\phi\, dt\right]} \cdot \sum_0^{\infty} \exp\left\{-\beta_n^2 \int_o^t \phi\, dt\right\} \frac{J_o(\beta_n r)}{J_o^2(\beta_n a)} \qquad (4.7)$$

d) negligible longitudinal diffusion:

$$C = \frac{N}{\pi a^2} \sum_0^{\infty} \exp\left\{-\beta_n^2 \int_o^t \phi\, dt\right\} \cdot \frac{J_o(r\beta_n)}{J_o^2(a\beta_n)} \qquad (4.8)$$

where β_n is defined by the equation below:

$$J_1(\beta_n a) = 0 \qquad (4.9)$$

The preceding four solutions (equations (4.5) to (4.8)) are identical with those that would be obtained by solving equation (4.1) if it is assumed that D = constant if one substitutes in the final expression

$$Dt = \int_0^t \Phi \, dt \qquad (4.10)$$

Hence an eddy diffusivity, E, analogous to D may be defined as

$$E = \frac{1}{t} \int_0^t \Phi \, dt \qquad (4.11)$$

Unlike molecular diffusion from a fixed point source, E will vary with time.

Diffusion From a Continuous Source:

Theory presented upto this point has been for isotropic, homogeneous turbulence, conditions which at best can be only approximated. The experimental system used in this research consists of diffusion from a continuous source of material located in the center of a particulate fluidized bed through which fluid is flowing in the Z-direction. The fluid velocity is substantially uniform in the cross section of the container. It has been assumed therefore that the field may be considered homogeneous and isotropic in the radial direction.

The equations developed above may be used if the system is represented as a number of instantaneous sources which are carried downstream with the fluid. Each one of these sources will spread out equally in all directions and thus consists of a spherical cloud of the material which increases in radius as it is transported downstream. The case in which longitudinal

diffusion is neglected is represented by a number of sources which spread out only in the radial direction and therefore consists of a series of expanding discs.

At r=0 and at a distance Z' from the injection point is a source which has been in the field a time t=Z'/U. The concentration profile in a cross-section at a given value of Z will result from contribution of sources that have been in the field for times ranging from 0 to ∞. When longitudinal diffusion is neglected, only a source which has been in the field a time t=Z/U will contribute to the concentration profile at a longitudinal distance Z from the injector.

Case (i) Longitudinal Diffusion is not Neglected.

Equations (4.5) and (4.7) may be used to describe the contribution of a single source if the quantity (Ut-Z) is substituted for Z. The sum of the effect of all the sources is obtained in the following manner:

Wall effects unimportant

$$C = \int_0^{\infty} \frac{Q\,dt}{\left[2\pi \int_0^t 2\phi\,dt\right]^{3/2}} \cdot \exp\left\{ - \frac{r^2 + (Ut - Z)^2}{4 \int_0^t \phi\,dt} \right\} \qquad (4.12)$$

Wall effects important

$$C = \int_0^{\infty} \frac{Q\,dt \exp\left\{ - \frac{(Ut - Z)^2}{4 \int_0^t \phi\,dt} \right\}}{\pi a^2 \left[2\pi \int_0^t 2\phi\,dt\right]^{1/2}} \cdot \sum_0^{\infty} \exp\left\{ - \beta_n^2 \int_0^t \phi\,dt \right\} \frac{J_o(r\beta_n)}{J_o^2(a\beta_n)} \qquad (4.13)$$

Q = rate of flow of material from the injector

$= C_A \pi a^2 U.$

Case (ii) Longitudinal Diffusion is Neglected

Equations (4.6) and (4.8) may be used to describe a continuous source by substituting $t = Z/U$

Wall effects unimportant:

$$C = \frac{N}{(2\pi)\int_0^{Z/U} 2\phi\,dt} \exp\left\{ - \frac{r^2}{2\int_0^{Z/U} 2\phi\,dt} \right\} \qquad (4.14)$$

Wall effects important

$$C = \frac{N}{\pi a^2} \sum_0^{\infty} \exp\left\{ -\beta_n^2 \int_0^{Z/U} \phi\,dt \right\} \cdot \frac{J_o(r\beta_n)}{J_o^2(a\beta_n)} \qquad (4.15)$$

* * *

EXPERIMENTAL DATA, RESULTS AND DISCUSSIONS

Data Collection:

Experiments were conducted over the flow rate range from 6 to 13 LPM (velocity range from 3.725 to 8.072 cm/sec.) encompassing fractions void between 0.56 and 0.70 thereby maintaining the dense-phase characteristic of the fluidized bed. Most of the studies were conducted with a bed weighting 450 gm over the above mentioned velocity range. But some of the investigations were also carried out with beds weighting 150 gm, 250 gm. and 350 gm. respectively at one particular flow rate, that is, 8 LPM.

Reduction of Data

The experiments carried out in this investigation were such that diffusion in the flow direction could not be measured. Therefore the equations (4.14) and (4.15) developed for a continuous source when longitudinal diffusion is neglected were used in examining the data.

The equations (4.14) and (4.15) can be re-written in the following forms:

Wall effects unimportant:

$$\frac{C}{C_A} = \frac{a^2}{4\int_0^{Z/U} \phi\, dt} \exp\left\{-\frac{r^2}{4\int_0^{Z/U} \phi\, dt}\right\} \quad (5.1)$$

Wall effects important:

$$\frac{C}{C_A} = \sum_{0}^{\infty} \exp \left\{ -\beta_n^2 \int_0^{Z/U} \phi \, dt \right\} \cdot \frac{J_o (r \beta_n)}{J_o^2 (a \beta_n)} \qquad (5.2)$$

Denoting $\int_0^{Z/U} \phi \, dt$ in the above two equations by B_1 and B_2 respectively the above equations become:

Wall effects unimportant:

$$\frac{C}{C_A} = \frac{a^2}{4 B_1} \exp\left\{ - \frac{r^2}{4 B_1} \right\} \qquad (5.3)$$

Wall effects important:

$$\frac{C}{C_A} = \sum_{0}^{\infty} \exp \left\{ - \beta_n^2 B_2 \right\} \cdot \frac{J_o (r \beta_n)}{J_o^2 (a \beta_n)} \qquad (5.4)$$

For the case r = 0.0, the equations are further simplified to the following forms:

Wall effects unimportant:

$$(C/C_A)_o = \frac{a^2}{4 B_1} \qquad (5.5)$$

Wall effects important:

$$(C/C_A)_o = \sum_{0}^{\infty} \exp \left\{ - \beta_n^2 B_2 \right\} \cdot \frac{1}{J_o^2 (a \beta_n)} \qquad (5.6)$$

In Chapter IV, Eddy Diffusivity was defined as

$$E = \frac{1}{t} \int_o^t \phi \, dt \qquad (4.11)$$

which may be re-written as

$$E = \frac{U}{Z} \int_o^{Z/U} \phi \, dt \qquad (5.7)$$

In keeping with the notations used earlier, the above leads to the following:

$$E_1 = \frac{U}{Z} B_1 \qquad (5.8)$$

$$E_2 = \frac{U}{Z} B_2 \qquad (5.9)$$

Again, Peclet Number is defined as

$$N_{Pe} = D_p U/E \qquad (5.10)$$

which further leads to the following:

$$N_{Pe_1} = D_p U/E_1 = D_p Z/B_1 \qquad (5.11)$$

$$N_{Pe_2} = D_p U/E_2 = D_p Z/B_2 \qquad (5.12)$$

Computer Programs were written for the equations (5.3) and (5.4) in order to evaluate B_1 and B_2 and consequently E_1, E_2, N_{Pe_1} and N_{Pe_2} were also computed. The programs are shown in Appendices II and III respectively. The input data consisted of "C/C_A" values, the "Z" values, the "r" values and the "U" values.

Tabulation of Results and Drawing of Plots:

Transmittance values, the computed C and C/C_A values, the r values, the computed B_1, B_2, E_1, E_2, N_{Pe_1} and N_{Pe_2} values are tabulated in Tables 5.3 to 5.22.

Table 5.3 describes the results for the 150 -gm bed at ϵ =0.58 and Z = 2.475 cm.

Tables 5.4 and 5.5 describe the results for the 250 -gm bed at ϵ=0.58 and Z = 2.475 cm and 6.285 cm. respectively.

Tables 5.6, 5.7 and 5.8 describe the results for the 350 gm bed at ϵ =0.58 and Z = 2.475 cm., 6.285 cm. and 10.095 cm. respectively.

Tables 5.9, 5.10, 5.11 and 5.12 describe the results for the 450 gm bed at ϵ = 0.58 and Z = 2.475 cm., 6.285 cm, 10.095 cm and 13.905 cm. respectively.

Tables 5.13 and 5.14 describe the results for the 450 gm bed at ϵ =0.57 and Z =2.475 cm. and 6.285 cm. respectively.

Tables 5.15 to 5.22 describe the results for the 450 gm bed at Z = 10.095 cm and ϵ = 0.56 (U = 3.72 cm/sec), 0.56 (U = 4.34 cm/sec.), 0.57, 0.61, 0.637, 0.662, 0.682 and 0.701 respectively,

Figures 5.3 to 5.22 show the radial concentration - profiles for the respective tables mentioned above. Individual experimental points are used twice, as original points and as reflected points on the other lobe of the curve.

Figure 5.23 shows the B Vs. Z plot for the 450 gm. fluidized bed at ϵ = 0.58. The values were taken from the Tables 5.9, 5.10, 5.11 and 5.12. The B values were the center-line values.

Figure 5.24 shows the B vs. t plot for the same bed at the same void fraction, the values being taken from the same Tables viz. 5.9 to 5.12.

Figure 5.25 shows the B vs. $(C/C_A)_o$ plot at Z = 10.095 cm. at different fractions void. The values were taken from Tables 5.15, 5.16, 5.17, 5.11, 5.18, 5.19, 5.20, 5.21 and 5.22. The fractions void varied from 0.56 to 0.701. Each point in the plot corresponds

to a particular velocity of flow, that is, a particular void fraction.

Figure 5.26 shows the modified Peclet Number vs. modified Reynolds Number plot. Table 5.23 shows the values plotted in this figure. These values were derived from the same tables as mentioned in the above para.

Discussions:

Figure 5.2 which is a log-log plot of pressure drop vs. fluid velocity can be divided into three regions - Fixed bed, Incipient fluidization and Fluidized bed. The segment AB corresponds to the fixed bed and shows that as the velocity rises, the pressure drop in the fluid passing through the bed increases. Eventually the pressure drop equals the force of gravity on the particles and the particles begin to move. This is at point B on the graph. First the bed expands slightly with the particles still in contact. The porosity increases, and the pressure drop rises more slowly than before. When the point C is reached, the bed is in the loosest possib condition with the particles still in contact. As the velocity is still further increased, the particles separate and true fluidization begins. The pressure drop diminishes a little from point C to D. From point D onward the particles move more and more vigorously, swirling about and travelling in random directions. The segment BCD corresponds to incipient fluidization and is also called intermediate region. The region beyond D is the fluidized bed region.

It is seen from Figures 5.3, 5.4, 5.6, 5.9 and 5.13 which are radial concentration profiles at Z = 2.475 cm., that the peaks of the curves lie somewhere between C/C_A = 10 and 14 and the lowest points somewhere between C/C_A = 0 and 0.55.

At Z = 6.285 cm., as in Figures 5.5, 5.7, 5.10 and 5.14, the peaks of the curves lie somwhere between C/C_A = 5 and 7 and the lowest points somewhere between C/C_A = 0.47 and 0.97.

At Z = 10.095 cm., as in Figures 5.8 and 5.11 the peaks of the curves lie somewhere between C/C_A = 3 and 4 and the lowest points somewhere between C/C_A = 1.0 and 1.6.

At Z = 13.905 cm., as in Figure 5.12, the peak of the curve lies at C/C_A = 2.797 and the lowest point at C/C_A = 1.494.

Thus from the above discussion of Figures 5.3 to 5.14 it can be concluded that, provided the fluid velocity remains more or less constant, the center-line tracer compositions decrease and the near-to-the-wall tracer compositions increase downstream.

Figures 5.11 and 5.15 to 5.22 show not only the effect of increasing velocity on the tracer distribution at a fixed value of Z = 10.095 cm. but also the transition from fixed bed to fluidized bed. Figure 5.15 corresponds to a fluid flow rate which lies very well in the fixed bed region of the curve in Figure 5.2. Thus the curve in Figure 5.15 is a fixed bed concentration profile. Figure 5.16 corresponds to a flow rate which is represented by point B in Figure 5.2. Thus the curve in Figure 5.16 is the concentration profile for a bed which is just at the start of incipient fluidi-

zation. Figure 5.17 corresponds to a flow rate which is represented by point C in Figure 5.2 which again lies in the"intermediate region." Likewise, Figure 5.11 corresponds to the flow rate represented by point D in Figure 5.2 which indicates the end of intermediate zone and the transition from fixed to fluidized bed is complete.

From Figures 5.15, 5.16 and 5.17 it is observed that the center-line compositions as well as the near-to-the-wall compositions increase with increasing velocity. But the pattern changes in Figure 5.11 and Figures5.18 to 5.22 which represent the fully fluidized state. The center-line composition starts decreasing as soon as the flow rate changes from 7.5 LPM to 8 LPM. From then onward the center-line compositions keep on decreasing while the near-to-the-wall compositions keep on increasing with increasing fluid velocity. The curves get flattened gradually with increasing velocity.

In Tables 5.3 to 5.22 it is seen that the computed values of B_1 and B_2 from Equations (5.5) and (5.6) for center-line compositions are identical. As a consequence, in these cases $E_1=E_2$ and $N_{Pe_1} = N_{Pe_2}$. For other radial positions, B_1 and B_2 differ and in some cases they are almost identical. Dashes occurring in the tables indicate that no computation was possible.

Figure 5.23 shows the nearly linear variation of B with Z at a constant fluid velocity. Figure 5.24 shows a similar linear variation of B with time of diffusion at a constant fluid velocity.

Figure 5.25 shows the variation of B with the center-line composition at Z = 10.095 cm. at different fluid velocities.

dotted-line curve indicates the variation of B with center-line composition starting from the fixed bed region. The first point corresponds to the flow rate of 6 LPM. The second and third correspond to 7 and 7.5 LPM respectively. From 7.5 LPM with increasing flow rate the curve takes a turn and follows the path shown by the heavy-line. The respective points on this heavy-line curve are those corresponding to flow rates of 8, 9, 10, 11, 12 and 13 LPM. Thus in transition from fixed bed to fluidized bed, B first decreases while center-line composition increases as shown by the dotted-line curve. B then increases while center-line composition decreases as shown by the heavy-line curve. The heavy-line curve stands for the fluidized state.

Figure 5.26 shows the variation of modified Peclet group as fluid velocity (Reynolds number) is increased. The curve starts from a fixed bed region (F = 6 LPM). The Peclet number increases sharply as the flow rate increases and attains a peak at 8 LPM. With further increase in flow rate the Peclet number has a steep fall. From 9 LPM to 12 LPM the fall in Peclet number is less steep. From 12 LPM to 13 LPM there is again a steep fall.

From a survey of the results in the tables 5.3 to 5.22 it is also found that at substantial distances from the source the concentration gradients in the flow direction are smaller than in the radial direction. In such cases diffusion is described by a Gaussian type of curve (Equation 5.3). However, close to the source the radial concentration profiles diverge from a Guassian distribution at large values of r, probably because of longitudinal diffusion.

An important experimental finding also deserves emphasis. It is that in most of the tables a good number of the radial values of B (or E) agree with each other. This leads to the conclusion that E is not dependent on 'r'. If some of radial values are inconsistent, it is not so much the effect of radial position. There may be other factors responsible for it like the orientation of particles and the wall-generated eddies. The particles used in the investigation were not spherical but more or less cylindrical. In a fluidized bed where the particles are in random motion, the non-spherical particles will have different orientations because of their geometry.

Another important conclusion is worth mentioning. It is the nature of mixing in the fluidized bed of the non-spherical particles used in this investigation. Figure 5.26 shows that the bed in passing through a fixed bed state to the fluidized bed state first exhibits a slow decrease in mixing in the fixed bed region. The mixing falls more rapidly in the 'intermediate region' till it attains a minimum at a void fraction of 0.58 (flow rate of 8 LPM). From then onward, in the fluidized state, the mixing increases very rapidly upto a void fraction of 0.61. The increase in mixing is less rapid in the void fractions range of 0.61 to 0.68. Beyond a fraction void of 0.68 the increase is again rapid till it reaches the void fraction of 0.70.

TABLE 5.1

ROTAMETER CALIBRATION DATA

F (LPM)	ΔF (LPM)
0.0	0.0
6.0	5.7
7.0	6.65
8.0	7.6

TABLE 5.2

PRESSURE DROP VERSUS FLOW RATE DATA

450 GM BED

F (LPM)	I_m (Cm)	AF (LPM)	U (Cm/Sec)	PD (gmf/Cm^2)	log (PD)	log U
2.0	24.15	1.9	1.242	14.49	2.673	0.2166
3.0	24.65	2.85	1.863	14.79	2.694	0.6221
4.0	25.35	3.8	2.484	15.21	2.722	0.9097
5.0	26.05	4.75	3.105	15.63	2.749	1.133
6.0	27.60	5.7	3.725	16.56	2.807	1.315
6.5	28.15	6.175	4.036	16.89	2.827	1.395
7.0	28.55	6.65	4.346	17.13	2.841	1.469
7.5	28.20	7.125	4.657	16.92	2.828	1.538
8.0	28.50	7.6	4.967	17.10	2.839	1.603
8.5	28.65	8.075	5.278	17.19	2.844	1.664
9.0	28.70	8.55	5.588	17.22	2.846	1.721
9.5	28.80	9.025	5.899	17.28	2.850	1.775
10.0	28.90	9.5	6.209	17.34	2.853	1.826
10.5	28.95	9.975	6.52	17.37	2.855	1.875
11.0	29.05	10.45	6.83	17.43	2.858	1.921
11.5	29.15	10.92	7.141	17.49	2.862	1.966
12.0	29.15	11.4	7.451	17.49	2.862	2.008
12.5	29.20	11.88	7.761	17.52	2.863	2.049
13.0	29.20	12.35	8.072	17.52	2.863	2.088
13.5	29.25	12.82	8.382	17.55	2.865	2.126
14.0	29.25	13.30	8.693	17.55	2.865	2.162

TABLE 5.3

ION DAT[illegible] C[illegible]UTED VALUES

150 GM Bed

Z = 2.475 CM

F = 8 LPM

T_A = 6[illegible] 0% ; C_A = 0.002311(gm/lit.); U = 4.96 (Cm./sec.); ϵ = 0.58

T %	C (gm./lit.)	C/C_A	r (Cm.)	B_1 (Cm^2)	B_2 (Cm^2)	E_1 (Cm^2/Sec)	E_2 (Cm^2/Sec)	N_{Pe_1}	N_{Pe_2}
1.0	0.02385	10.32	0.0	0.1965	0.1965	0.3938	0.3938	5.857	5.857
4.0	0.01667	7.213	0.2117	0.2700	0.2700	0.5411	0.5411	4.262	4.262
9.0	0.01247	5.396	0.423	0.3290	0.3285	0.6593	0.6583	3.498	3.503
36.8	0.005177	2.24	0.635	0.799	0.8000	1.601	1.603	1.44	1.439
55.5	0.003049	1.319	0.846	1.348	1.442	2.701	2.89	0.8538	0.7981
88.0	0.000662	0.2864	1.058	6.803	-	13.63	-	0.1692	-
97.0	0.0001577	0.06825	1.27	29.36	-	58.84	-	0.0392	-

TABLE 5.4

DIFFUSION DATA AND COMPUTED VALUES

250 GM Bed

Z = 2.475 CM

F = 8 LPM

ϵ = 0.58

T_A = 68.0%; C_A = 0.001997(gm/Lit); U=4.96 (Cm/sec.)

T %	C (gm/lit.)	C/C_A	r (Cm)	B_1 (Cm^2)	B_2 (Cm^2)	E_1 (Cm^2/sec)	E_2 (Cm^2/sec.)	N_{Pe_1}	N_{Pe_2}
1.5	0.02175	10.89	0.0	0.1865	0.1865	0.3738	0.3738	6.171	6.171
3.0	0.01816	9.092	0.2117	0.212	0.2117	0.4249	0.424	5.429	5.436
9.8	0.01203	6.023	0.423	0.2890	0.2885	0.5792	0.5782	3.982	3.989
60.0	0.002645	1.325	0.635	1.428	1.522	2.862	3.05	0.8059	0.7562
87.0	0.0007212	0.3611	0.846	5.44	-	10.9	-	0.2116	-
89.8	0.0005571	0.279	1.058	6.991	-	14.01	-	0.1646	-
92.0	0.0004318	0.2162	1.27	8.978	-	17.99	-	0.1282	-

TABLE 5.5

DIFFUSION DATA AND COMPUTED VALUES

250 GM Bed

Z = 6.285 CM

F = 8 LPM

T_A = 68.0%; C_A = 0.001997 (gm/lit.); U = 4.96 (Cm/sec.) ϵ = 0.53

T %	C (gm/lit)	C/C_A	r (Cm)	B_1 (Cm^2)	B_2 (Cm^2)	E_1 (Cm^2/sec)	E_2 (Cm^2/sec)	N_{Pe_1}	N_{Pe_2}
5.5	0.015[illegible]02	7.521	0.0	0.27	0.27	0.2131	0.2131	10.82	10.82
15.0	0.009624	4.919	0.2117	0.402	0.4013	0.3173	0.3167	7.27	7.283
35.5	0.005363	2.685	0.423	0.71	0.71	0.5603	0.5603	4.116	4.116
21.0	0.008088	4.047	0.635	0.387	0.3864	0.3054	0.3049	7.552	7.563
15.0	0.009824	4.919	0.846	–	–	–	–	–	–
46.0	0.004021	2.013	1.058	0.66	0.661	0.5209	0.5216	4.428	4.421
56.0	0.003003	1.503	1.27	0.225	0.225	0.1776	0.1776	12.99	12.99
58.0	0.002821	1.412	1.481	–	–	–	–	–	–
69.0	0.001922	0.9621	1.692	0.4916	0.4885	0.3875	0.3855	5.952	5.983

TABLE 5.6

DIFFUSION D T. AND COMPUTED VALUES

350 GM Bed

Z = 2.475 CM

F = 8 LPM

T_A = 68.0% ; C_A = 0.001997(gm./lit.); U = 4.96(Cm/Sec.) ϵ = 0.58

T %	C (gm./lit.)	C/C_A	r (Cm)	B_1 (Cm^2)	B_2 (Cm^2)	E_1 (Cm^2/Sec.)	E_2 (Cm^2/Sec.)	N_{Pe_1}	N_{Pe_2}
0.5	0.02744	13.74	0.0	0.1477	0.1477	0.2960	0.2960	7.792	7.792
2.0	0.02026	10.14	0.2117	0.1890	0.1885	0.3788	0.3778	6.089	6.105
11.2	0.01134	5.677	0.423	0.31	0.3095	0.6213	0.6203	3.713	3.718
12.2	0.01089	5.455	0.635	0.248	0.2477	0.497	0.4964	4.641	4.646
8.0	0.01306	6.549	0.846	–	–	–	–	–	–
65	0.002231	1.117	1.058	–	1.866	–	3.74	–	0.6168
84.5	0.000873	0.4367	1.27	0.1070	0.1068	0.2144	0.214	10.76	10.78
81	0.001091	0.5464	1.481	0.1820	0.1817	0.3647	0.3641	6.323	6.334

TABLE 5.

DIFFUSION DATA AND COMPUTED VALUES

350 GM Bed

Z = 6.285 CM

F = 8 LPM

T_A = 68.0%; C_A = 0.001997 (gm/lit.); U = 4.96(Cm/sec.); ϵ = 0.58

T %	C (gm./lit.)	C/C_A	r (Cm)	B_1 (Cm^2)	B_2 (Cm^2)	E_1 (Cm^2/Sec.)	E_2 (Cm^2/Sec)	N_{Pe_1}	N_{Pe_2}
10.0	0.01192	5.97	C.0	0.34	0.34	0.2683	0.2683	8.596	8.596
11.5	0.0112	5.608	0.2117	0.35	0.3566	0.277	0.2767	8.326	8.336
12.C	0.01098	5.498	0.423	0.322	0.321	0.2541	0.2533	9.076	9.104
18.0	0.00888	4.446	0.635	0.34	0.3391	0.2683	0.2676	8.596	8.618
48.0	0.003801	1.903	0.846	0.869	0.8725	0.6858	0.6886	3.363	3.350
48.0	0.003801	1.903	1.058	0.7260	0.7280	0.5729	0.5745	4.026	4.014
32.0	0.005901	2.954	1.27	-	-	-	-	-	-
70.0	0.001847	0.9248	1.481	0.2550	0.2545	0.2012	0.2008	11.46	11.48

TABLE 5.8

DIFFUSION DATA AND COMPUTED VALUES

350 GM Bed
Z = 10.095
F = 8 LPM

T_A = 68.0%; C_A = 0.001997(gm/lit.); U = 4.96 (cm/sec.) ; ϵ =0.58

T %	C (gm./lit.)	C/C_A	r (Cm)	B_1 (Cm^2)	B_2 (Cm^2)	E_1 (Cm^2/Sec.)	E_2 (Cm^2/Sec.)	N_{Pe_1}	N_{pe_2}
21.C	0.008082	4.047	0.0	0.5019	0.5019	0,2466	0.2466	9.353	9.353
22.C	0.007841	3.926	0.2117	0.506	0.5057	0.2486	0.2485	9.277	9.283
25.5	0.007077	3.543	0.423	0.527	0.5265	0.2589	0.2587	8.907	8.916
30.7	0.006115	3.062	0.635	0.553	0.5524	0.2717	0.2714	8.489	8.498
28.2	0.006555	3.282	0.846	0.392	0.392	0.1926	0.1926	11.97	11.97
35.0	0.005437	2.722	1.058	-	-	-	-	-	-
52.2	0.003367	1.686	1.27	.641	0.647	0.3164	0.3179	7.289	7.255
54.9	0.003105	1.555	1.481	-	-	-	-	-	-

TABLE 5.9

DIFFUSION DATA AND COMPUTED VALUES

450 GM Bed

Z = 2.475 CM

F = 8 LPM

T_A = 680%; C_A = 0.001997 (Gm/lit); U = 4.96 (Cm/sec.) ; ϵ = 0.58

f %	C (gm./lit)	C/C_A	r (Cm)	B_1 (Cm^2)	B_2 (Cm^2)	E_1 (Cm^2/sec.)	E_2 (Cm^2/Sec)	N_{Pe_1}	N_{Pe_2}
0.5	0.02744	13.74	0.0	0.1477	0.1477	0.296	0.296	7.792	7.792
0.8	0.025	12.52	0.2117	0.151	0.1505	0.3026	0.3016	7.622	7.647
2.0	0.02026	10.14	0.423	0.148	0.148	0.2966	0.2966	7.776	7.776
15.0	0.009824	4.919	0.635	0.293	0.2923	0.5872	0.5858	3.928	3.937
30.0	0.006235	3.122	0.846	0.429	0.428	0.8597	0.8577	2.683	2.689
44.5	0.004193	2.090	1.058	0.151	0.15	0.3026	0.3006	7.622	7.672
52.0	0.003386	1.696	1.27	0.273	0.2728	0.5471	0.5467	4.216	4.219
91.0	0.0004884	0.2445	1.481	0.133	0.1326	0.2665	0.2657	8.653	8.679

TABLE 5.10

DIFFUSION DATA AND COMPUTED VALUES

450 GM Bed
Z = 6.285 CM
F = 8 LPM

T_A = 66.5%; C_L = 0.002113 (gm./lit.); U = 4.96 (Cm/sec.); ϵ = 0.58

T %	C (gm/lit.)	C/C_A	r (Cm)	B_1 (Cm^2)	B_2 (Cm^2)	E_1 (Cm^2/sec.)	E_2 (Cm^2/sec)	N_{Pe_1}	N_{Pe_2}
10.0	0.01192	5.644	0.0	0.3599	0.3599	0.2840	0.2840	8.120	8.120
29.0	0.006110	3.034	0.2117	0.658	0.6579	0.5193	0.5192	4.442	4.442
25.0	0.007173	3.398	0.423	0.551	0.55	0.4348	0.4340	5.304	5.314
41.0	0.004617	2.185	0.635	0.822	0.8234	0.6487	0.6498	3.555	3.549
28.0	0.006592	3.120	0.846	0.429	0.4285	0.3386	0.3382	6.812	6.82
43.0	0.004371	2.069	1.058	0.629	0.629	0.4964	0.4964	4.646	4.646
67.0	0.002074	0.9816	1.27	1.61	-	1.271	-	1.815	-
76.0	0.001421	0.6727	1.481	-	0.2033	-	0.1604	-	14.38
82.0	0.001028	0.4864	1.692	-	0.2566	-	0.2025	-	11.39

TABLE 5.11

DIFFUSION DATA AND COMPUTED VALUES

450 GM Bed

Z = 10.095 CM

F = 8 LPM

T_A = 68.0% ; C_A = 0.001997 (gm./lit.); U = 4.96 (cm/Sec.), ϵ =0.58

T %	C (gm/lit.)	C/C_A	r (Cm.)	B_1 (Cm^2)	B_2 (Cm^2)	E_1 (Cm^2/sec)	E_2 (Cm^2/sec)	N_{Pe_1}	N_{Pe_2}
27.8	0.006629	3.319	0.0	0.6119	0.6119	0.3006	0.3006	7.671	7.671
29.0	0.006410	3.210	0.2117	0.622	0.621	0.3056	0.3051	7.547	7.559
30.0	0.006235	3.122	0.423	0.604	0.604	0.2968	0.2968	7.772	7.772
34.5	0.005511	2.759	0.635	0.627	0.6264	0.3081	0.3078	7.487	7.494
30.0	0.006235	3.122	0.846	0.429	0.428	0.2108	0.2103	10.94	10.97
41.0	0.004617	2.312	1.058	0.504	0.504	0.2476	0.2476	9.314	9.314
47.8	0.003823	1.914	1.27	–	–	–	–	–	–
66.0	0.002152	1.077	1.481	0.297	0.2969	0.1459	0.1459	15.81	15.81

TABLE 5.12

DIFFUSION DATA AND COMPUTED VALUES

450 GM Bed

Z = 13.905 CM

F = 8 LPM

T_A = 68.0%; C_A = 0.001997(gm/lit.); U = 4.96 (Cm/Sec.); = 0.58

T %	C (gm./lit)	C/C_A	r (Cm)	B_1 (Cm^2)	B_2 (Cm^2)	E_1 (Cm^2/sec)	E_2 (Cm^2/Sec)	N_{Pe_1}	N_{Pe_2}
34.0	0.005587	2.779	0.0	0.726	0.726	0.259	0.259	8.906	8.906
38.2	0.004984	2.495	0.2117	0.803	0.8029	0.2864	0.2864	8.052	8.052
46.0	0.004021	2.015	0.423	0.963	0.966	0.3435	0.3446	6.714	6.693
50.0	0.003590	1.797	0.635	1.024	1.032	0.3657	0.3683	6.314	6.262
51.0	0.003487	1.746	0.846	0.967	0.976	0.3449	0.3481	6.686	6.625
48.0	0.003801	1.903	1.058	0.726	0.728	0.259	0.2597	8.906	8.882
49.0	0.003694	1.850	1.27	0.423	0.424	0.1509	0.1512	15.29	15.25
55.0	0.003096	1.550	1.481	-	-	-	-	-	-
56.2	0.002984	1.494	1.692	-	-	-	-	-	-

TABLE 5.

DIFFUSION DATA AND COMPUTED VALUES

450 GM Bed

Z = 2.475 Cm

F = 7.5 LPM

T_A = 690%; C_A = 0.001922 (gm/lit); U = 4.65 (Cm/Sec); ϵ = 0.57

T %	C (gm./lit)	C/	r (Cm)	B_1 (Cm^2)	B_2 (Cm^2)	E_1 (Cm^2/Sec)	E_2 (Cm^2/Sec)	N_{Pe_1}	N_{Pe_2}
0.8	0.025	13.01	C.0	0.156	0.156	0.2913	0.2913	7.377	7.377
3.0	0.01813	9.45	0.2117	0.204	0.2032	0.3833	0.3818	5.642	5.664
2.0	0.02026	10.54	0.423	0.14	0.139	0.2630	0.2612	8.221	8.28
2.0	C.02026	10.54	0.635	-	-	-	-	-	-
23.0	C.007611	3.961	0.846	0.132	0.2519	0.2480	0.4733	8.719	4.569
52.0	0.003386	1.762	1.058	0.127	0.127	0.2386	0.2386	9.062	9.062
70.2	0.001852	0.9635	1.27	0.154	0.153	0.2893	0.2875	7.473	7.522
90.2	0.0005341	0.278	1.481	0.139	0.1383	0.2612	0.2598	8.26	8.322
94.8	0.0002765	0.1439	1.691	0.16	0.1598	0.3006	0.3002	7.193	7.202

TABLE 5.14

DIFFUSION DATA AND COMPUTED VALUES

450 GM Bed

Z = 6.285 Cm

F = 7.5 LPM

π_A = 64.0% ; C_A = 0.002311 (Gm/lit); U = 4.65 (Cm/sec) ; ϵ = 0.57

T %	υ (Gm./lit)	C/C_A	r (Cm.)	B_1 (Cm^2)	B_2 (Cm^2)	E_1 (Cm^2/Sec)	E_2 (Cm^2/Sec)	N_{Pe_1}	N_{Pe_2}
8.0	0.01308	5.659	0.0	0.3589	0.3589	0.2655	0.2655	8.143	8.143
10.0	0.01192	5.159	0.2117	0.3830	0.3821	0.2834	0.2827	7.631	7.64
11.0	0.01143	4.946	0.423	0.3630	0.3629	0.2686	0.2685	8.051	8.053
29.0	0.006410	2.774	0.635	0.6230	0.6225	0.4609	0.4606	4.691	4.695
34.0	0.005587	2.417	0.846	0.6340	0.6333	0.4691	0.4686	4.610	4.615
62.0	0.002476	1.071	1.058	-	2.150	-	1.591	-	1.359
47.0	0.003910	1.692	1.27	0.2720	0.271	0.2012	0.2005	10.74	10.78
58.0	0.002821	1.221	1.481	0.3560	0.3555	0.2634	0.2630	8.209	8.221
81.0	0.001091	0.4722	1.692	0.2530	0.2525	0.1872	0.1868	11.55	11.57

TABLE 5.15

DIFFUSION DATA AND COMPUTED VALUES

450 GM Bed

Z = 10.095 CM

F = 6.0 LPM

T_b = 67.0% ; C_A = 0.002074 (gm./lit) ; U = 3.72 (cm/sec) ; ϵ = 0.56

T %	C (gm./lit)	C/C_A	r (Cm)	B_1 (Cm^2)	B_2 (Cm^2)	E_1 (Cm^2/sec)	E_2 (Cm^2/sec)	N_{Pe_1}	N_{Pe_2}
29.0	0.00641	3.091	0.0	0.657	0.657	0.2421	0.2421	7.145	7.145
37.0	0.005149	2.483	0.423	0.772	0.772	0.2845	0.2845	6.081	6.081
41.5	0.004554	2.196	0.635	0.818	0.8185	0.3014	0.3016	5.739	5.735
49.0	0.003694	1.781	0.846	0.943	0.951	0.3475	0.3505	4.978	4.936
64.0	0.002311	1.114	1.058	1.515	1.881	0.5583	0.6931	3.098	2.496
72.0	0.001701	0.8203	1.27	0.141	-	0.05196	-	33.29	-
78.0	0.001287	0.6204	1.481	0.195	0.1941	0.07186	0.07153	24.07	24.18

TABLE 5.16

DIFFUSION DATA AND COMPUTED VALUES

450 GM Bed

Z = 10.095 Cm

F = 7.0 LPM

T_A = 66.0% ; C_A = 0.002152 (gm/lit); U = 4.34 (cm/sec) ; ϵ = 0.56

T %	C (Gm/lit)	C/C_A	r (Cm)	B_1 (Cm^2)	B_2 (Cm^2)	E_1 (Cm^2/sec)	E_2 (Cm^2/sec)	N_{Pe_1}	N_{Pe_2}
27.0	0.006781	3.151	0.0	0.644	0.644	0.2769	0.2769	7.289	7.289
31.0	0.006065	2.819	0.2117	0.709	0.709	0.3048	0.3048	6.621	6.621
49.2	0.003573	1.707	0.423	1.144	1.153	0.4918	0.4978	4.103	4.054
56.5	0.002957	1.374	0.635	1.373	1.445	0.5903	0.6212	3.413	3.249
68.8	0.001937	0.900	0.846	2.069	-	0.8895	-	2.269	-
63.0	0.002393	1.112	1.058	1.519	1.80	0.6530	0.8125	3.090	2.484
70.8	0.001703	0.831	1.27	1.997	-	0.8585	-	2.351	-
80.2	0.001143	0.531	1.481	3.226	-	1.387	-	1.455	-

TABLE 5.17

DIFFUSION DATA AND COMPUTED VALUES

450 GM Bed

Z = 10.095 CM

F = 7.5 LPM

T_A = 65.0% ; C_A = 0.002231 (gm/lit); U = 4.65 (cm/sec); ϵ = 0.57

m	C (gm/lit)	C/C_A	r (Cm)	B_1 (Cm^2)	B_2 (Cm^2)	E_1 (Cm^2/sec)	E_2 (Cm^2/sec)	N_{Pe_1}	N_{Pe_2}
20.0	0.008335	3.736	0.0	0.5435	0.5435	0.2503	0.2503	8.637	8.637
23.5	0.0075	3.362	0.2117	0.5930	0.5924	0.2732	0.2729	7.916	7.924
24.7	0.007242	3.246	0.423	0.5790	0.5790	0.2667	0.2667	8.107	8.107
32.8	0.005773	2.588	0.635	0.6760	0.6760	0.3114	0.3114	6.944	6.944
40.8	0.004643	2.081	0.846	0.7750	0.7760	0.3570	0.3574	6.057	6.049
51.0	0.003191	1.43	1.058	1.101	1.145	0.507	0.5274	4.264	4.10
51.2	0.003467	1.554	1.27	0.778	0.7890	0.3584	0.3634	6.034	5.95
67.2	0.002058	0.9227	1.481	0.2540	0.2540	0.1170	0.1170	18.48	18.48

TABLE 5.18

DIFFUSION DATA AND COMPUTED VALUES

450 GM Bed

Z = 10.095Cm

F = 9.0 LPM

T_A = 58.0% ; C_A = 0.002821 (gm/lit.) ; U = 5.56 (Cm/sec); ϵ = 0.61

T %	C (gm/lit)	C/C_A	r (Cm)	B_1 (Cm^2)	B_2 (Cm^2)	E_1 (Cm^2/sec)	E_2 (Cm^2/sec)	N_{Pe_1}	N_{Pe_2}
17.0	0.009176	3.253	0.0	0.624	0.624	0.3437	0.3437	7.523	7.523
18.0	0.00888	3.148	0.2117	0.634	0.6335	0.3492	0.3489	7.404	7.41
24.0	0.00739	2.62	0.423	0.729	0.729	0.4015	0.4015	6.439	6.439
28.0	0.006592	2.337	0.635	0.761	0.7615	0.4191	0.4194	6.168	6.164
35.0	0.005437	1.927	0.846	0.855	0.8585	0.4709	0.4728	5.49	5.468
38.0	0.005011	1.776	1.058	0.809	0.814	0.4456	0.4483	5.802	5.767
46.0	0.004021	1.426	1.27	0.918	0.948	0.5056	0.5221	5.113	4.952
48.0	0.003801	1.347	1.481	0.639	0.66	0.3519	0.3635	7.346	7.112

TABLE 5.19

DIFFUSION DATA AND COMPUTED VALUES

450 GM Bed

Z = 10.095 Cm

F = 10.0 LPM

T_A = 61.5 %; C_A = 0.002517 (gm./lit); U = 6.2 (Cm/sec) ; ϵ = 0.637

T %	C (gm./lit)	C/C_A	r (Cm)	B_1 (Cm^2)	B_2 (Cm^2)	E_1 (Cm^2/sec)	E_2 (Cm^2/sec)	N_{Pe_1}	N_{Pe_2}
22.0	0.007841	3.115	0.0	0.6519	0.6519	0.4004	0.4004	7.201	7.201
23.0	0.007611	3.023	0.2117	0.6610	0.66	0.406	0.4053	7.102	7.112
26.0	0.006976	2.771	0.423	0.6870	0.686	0.4219	0.4213	6.833	6.843
26.5	0.006877	2.732	0.635	0.6340	0.634	0.3894	0.3894	7.404	7.404
34.0	0.005587	2.219	0.846	0.712	0.7124	0.4373	0.4375	6.593	6.589
35.0	0.005437	2.160	1.058	0.581	0.5809	0.3568	0.3568	8.079	8.081
41.5	0.004554	1.809	1.27	0.505	0.506	0.3102	0.3108	9.295	9.277
51.0	0.003487	1.385	1.481	-	-	-	-	-	-
55.0	0.003096	1.23	1.692	-	-	-	-	-	-

TABLE 5.20

DIFFUSION DATA AND COMPUTED VALUES

450 GM Bed

Z = 10.095 CM

F = 11.0 LPM

T_A = 64.0%; C_A = 0.002311 (gm/lit); U = 6.81 (Cm/sec); ϵ = 0.662

T %	C (gm/lit)	C/C_A	r (Cm)	B_1 (Cm^3)	B_2 (Cm^3)	E_1 (Cm^2/sec)	E_2 (Cm^2/sec)	N_{Pe_1}	N_{Pe_2}
26.3	0.006928	2.999	0.0	0.6760	0.6760	0.456	0.456	6.944	6.944
27.0	0.006781	2.934	0.2117	0.6810	0.6807	0.4594	0.4592	6.893	6.896
29.5	0.006322	2.735	0.423	0.6970	0.6960	0.4702	0.4695	6.735	6.745
35.0	0.005437	2.352	0.635	0.7560	0.7560	0.51	0.51	6.209	6.209
48.0	0.003801	1.645	0.846	1.039	1.055	0.7009	0.7117	4.518	4.449
47.0	0.00391	1.692	1.058	0.87	0.879	0.5869	0.5930	5.396	5.34
49.0	0.003694	1.598	1.27	0.733	0.74	0.4945	0.4992	6.404	6.343
68.0	0.001997	0.8642	1.481	0.241	0.2407	0.1626	0.1624	19.48	19.5

TABLE 5.21

DIFFUSION DATA AND COMPUTED VALUES

450 GM Bed

Z = 10.095 Cm

F = 12.0 LPM

T_A = 66.0% ; C_A = 0.002152 (gm./lit); U = 7.42 (cm/sec); ϵ = 0.682

T %	C (gm/lit)	C/C_A	r (Cm)	B_1 (Cm^2)	B_2 (Cm^2)	E_1 (Cm^2/sec)	E_2 (Cm^2/Sec)	N_{Pe_1}	N_{Pe_2}
30.0	0.006235	2.898	0.0	0.700	0.700	0.5145	0.5145	6.706	6.706
38.5	0.004943	2.297	0.2117	0.873	0.8734	0.6417	0.6420	5.377	5.375
51.0	0.003487	1.621	0.423	1.207	1.228	0.8872	0.9026	3.889	3.823
35.0	0.005437	2.527	0.635	0.695	0.695	0.5108	0.5108	6.754	6.754
39.0	0.004876	2.266	0.846	0.692	0.6925	0.5086	0.5090	6,783	6.779
45.0	0.004135	1.922	1.058	0.714	0.7159	0.5248	0.5262	6.574	6.557
54.0	0.003191	1.483	1.27	0.854	0.8739	0.6277	0.6423	5.497	5.372
55.0	0.003096	1.439	1.481	-	-	-	-	-	-

TABLE 5.22

DIFFUSION DATA AND COMPUTED VALUES

450 GM Bed

Z = 10.095 Cm

F = 13.0 LPM

T_A = 65.0% ; C_A = 0.002231 (gm/lit); U = 8.04 (Cm/sec); ϵ = 0.701

T %	C (gm/lit)	C/C_A	r (Cm)	B_1 (Cm^2)	B_2 (Cm^2)	E_1 (Cm^2/sec)	E_2 (Cm^2/sec)	N_{Pe_1}	N_{Pe_2}
34.0	0.005587	2.504	0.0	0.811	0.811	0.6459	0.6459	5.788	5.788
36.2	0.005262	2.359	0.2117	0.850	0.850	0.677	0.677	5.523	5.523
36.0	0.005291	2.372	0.423	0.810	0.8105	0.6451	0.64551	5.795	5.792
38.0	0.005011	2.246	0.635	0.797	0.7975	0.6348	0.6352	5.890	5.886
39.0	0.004876	2.186	0.846	0.7260	0.7269	0.5782	0.5789	6.466	6.458
43.0	0.004371	1.959	1.058	0.6920	0.693	0.5511	0.5519	6.783	6.774
49.0	0.003694	1.656	1.27	0.6740	0.678	0.5368	0.540	6.965	6.924
53.0	0.003288	1.474	1.481	-	-	-	-	-	-
58.0	0.002821	1.265	1.692	-	-	-	-	-	-

TABLE 5.23

PECLET NUMBER VARIATION WITH REYNOLDS NO.

450 GM Bed

Z = 10.095 CM

F (LPM)	U (Cm/sec)	1-ε	ε	N'_{Re}	log N'_{Re}	N'_{Pe}
6.0	3.72	0.44	0.56	173.0	2.238	7.145
7.0	4.34	0.44	0.56	202.0	2.306	7.289
7.5	4.65	0.43	0.57	216.0	2.334	8.637
8.0	4.96	0.418	0.582	230.5	2.363	9.353
9.0	5.56	0.39	0.61	258.5	2.412	7.523
10.0	6.20	0.363	0.637	288.0	2.46	7.201
11.0	6.81	0.338	0.662	316.5	2.5	6.944
12.0	7.42	0.318	0.682	345.0	2.538	6.706
13.0	8.04	0.299	0.701	374.0	2.573	5.788

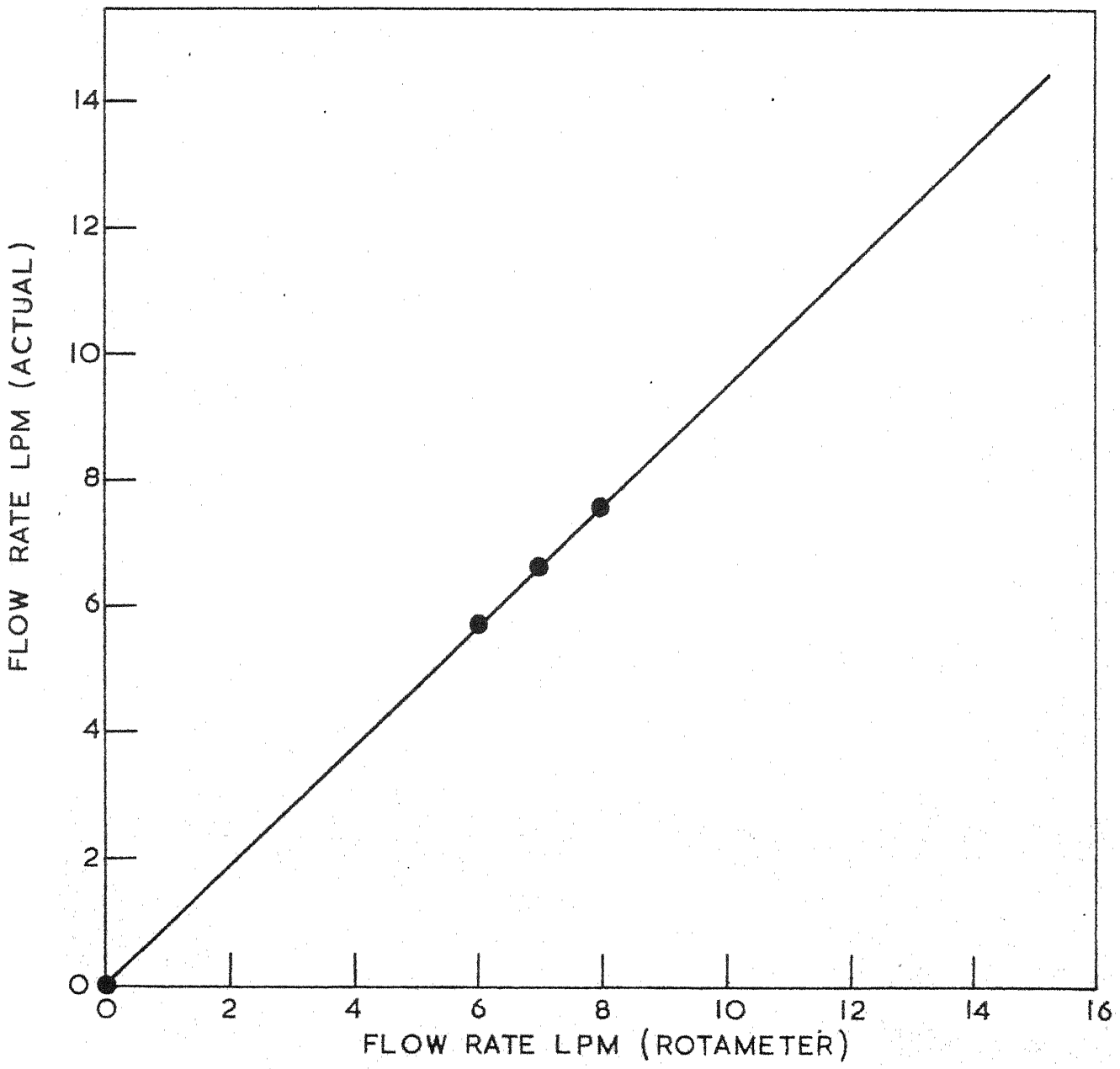

FIG. 5.1_ROTAMETER CALIBRATION GRAPH

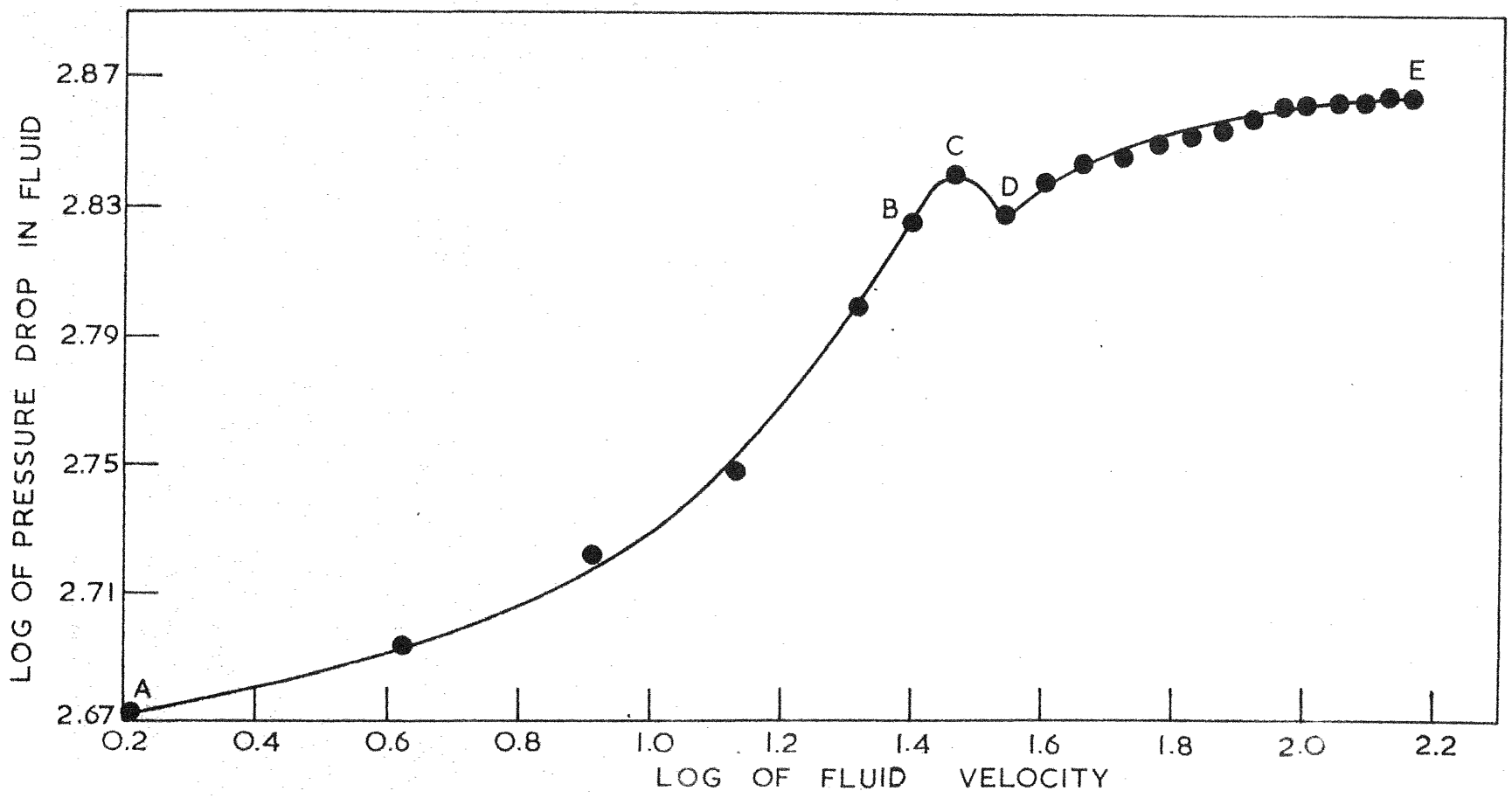

FIG. 5.2_PRESSURE DROP Vs. FLUID VELOCITY IN THE FLUIDIZED BED

TRACER DISTRIBUTION CURVES

● _ REFLECTED POINTS

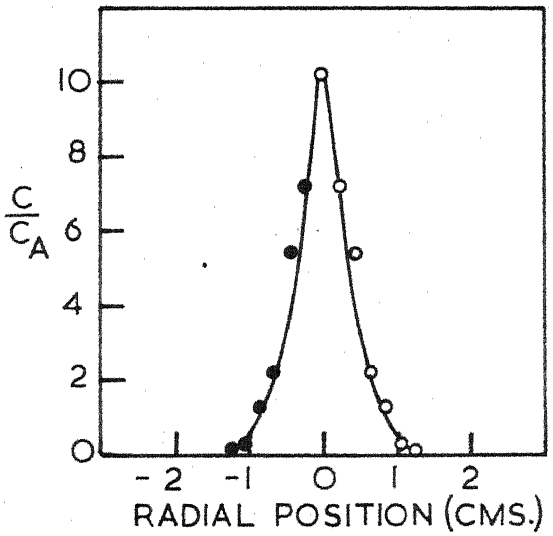

150 GMS. BED
Z = 2.475 CM.
F = 8 LPM

FIG._5.3

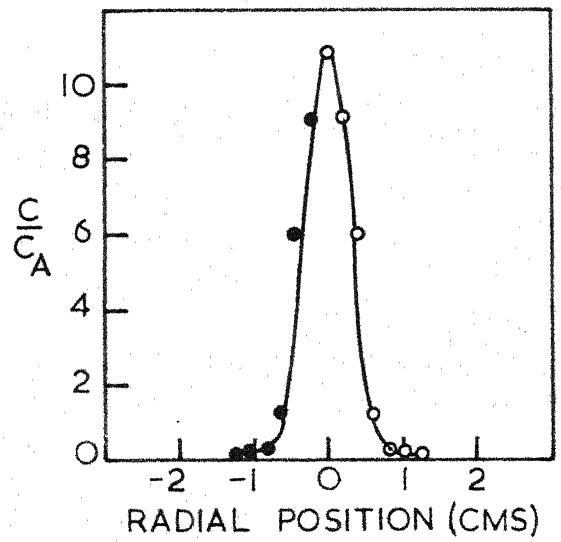

250 GMS. BED
Z = 2.475 CM.
F = 8LMP

FIG._5.4

TRACER DISTRIBUTION CURVES

● REFLECTED POINTS

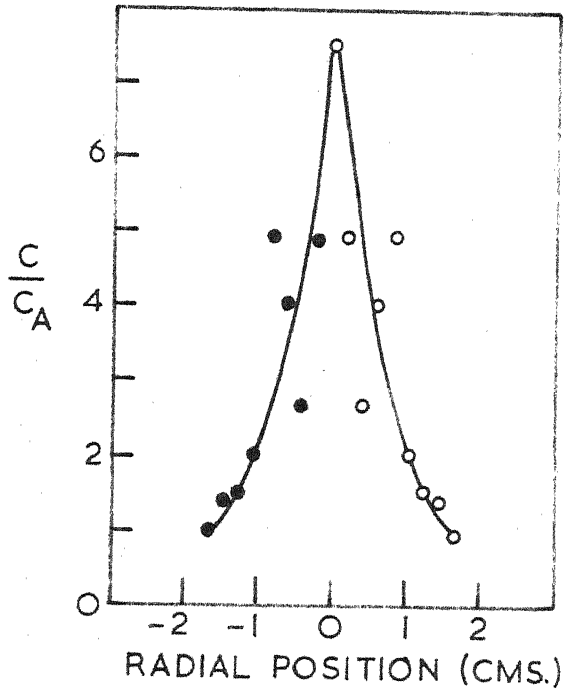

250 GMS BED
Z = 6.285 CM
F = 8 LPM

FIG_5.5

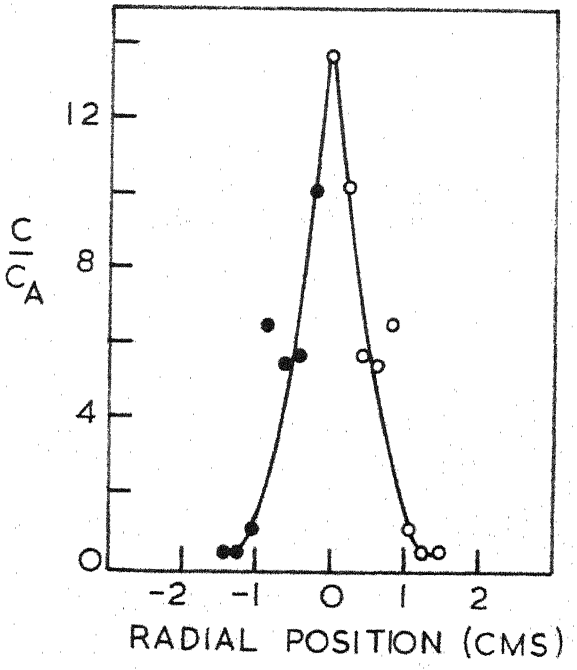

350 GMS BED
Z = 2.475 CM.
F = 8 LPM

FIG_5.6

TRACER DISTRIBUTION CURVES

● REFLECTED POINTS

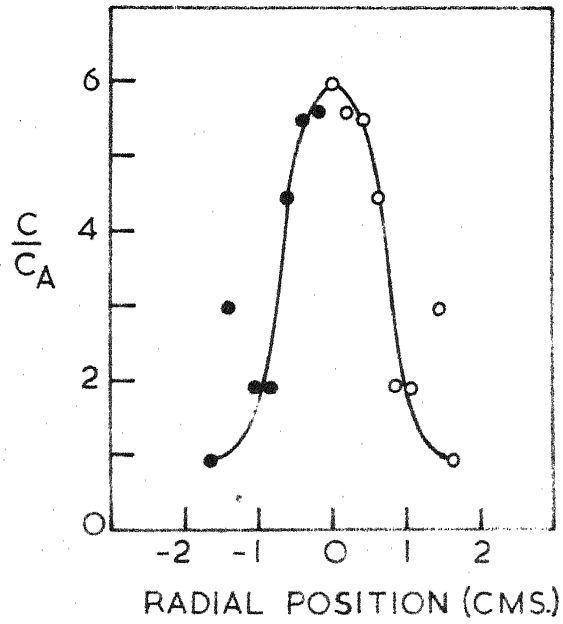

350 GMS BED
Z = 6.285 CM
F = 8 LPM

FIG. 5.7

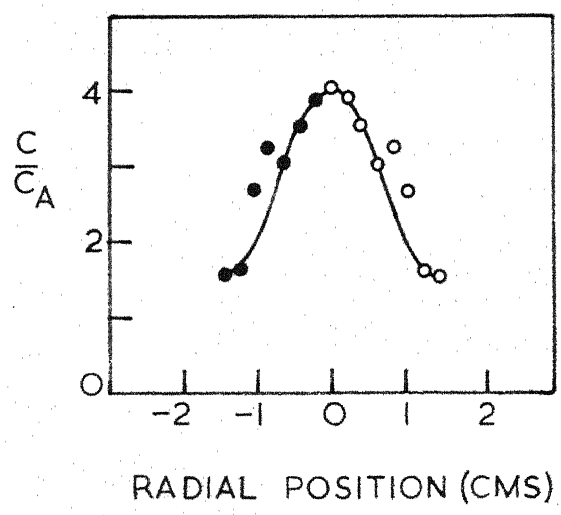

350 GMS BED
Z = 10.095 CM
F = 8 LPM

FIG. 5.8

TRACER DISTRIBUTION CURVES

● REFLECTED POINTS

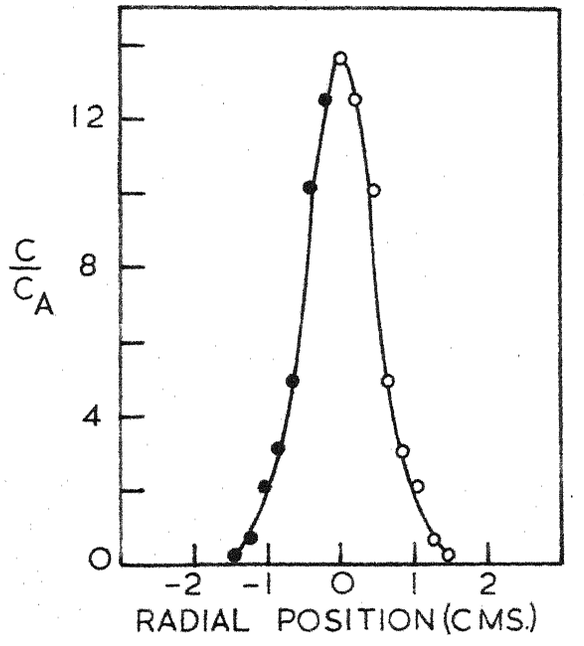

450 GMS BED
Z = 2.475 CM.
F = 8 LPM

FIG._5.9

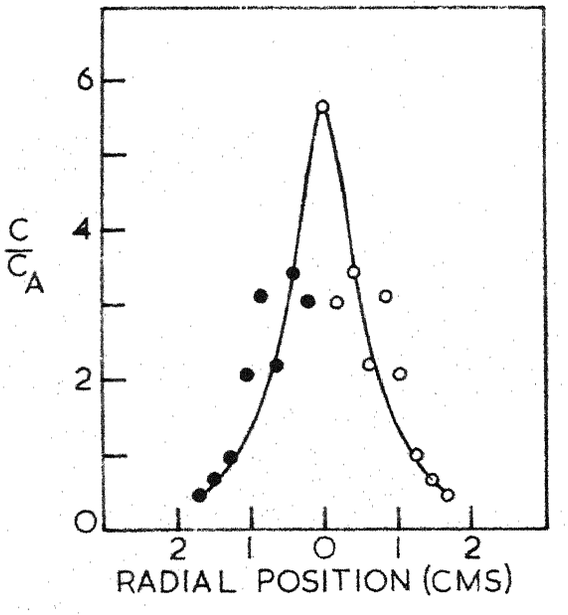

450 GMS BED
Z = 6.285 CM.
F = 8 LPM.

FIG._5.10

TRACER DISTRIBUTION CURVES

● REFLECTED POINTS

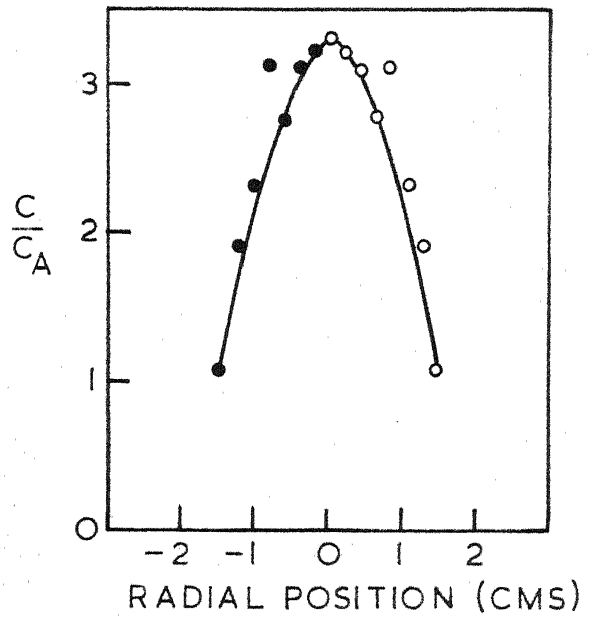

450 GMS BED
Z = 10.095 CM
F = 8 LPM

FIG_5.11

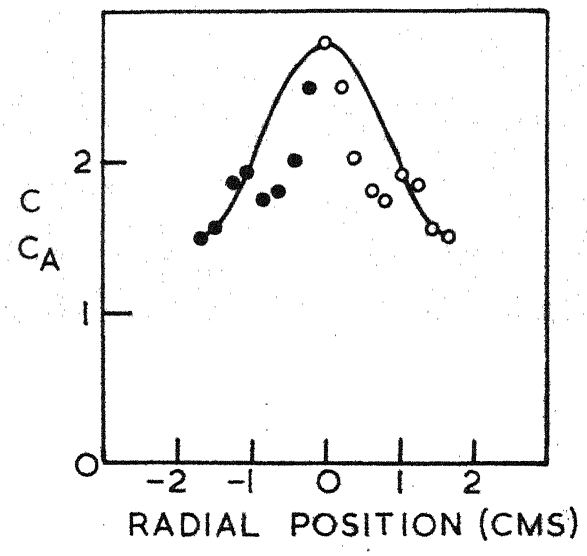

450 GMS. BED
Z = 13.905 CM
F = 8 LPM

FIG_5.12

TRACER DISTRIBUTION CURVES

● REFLECTED POINTS

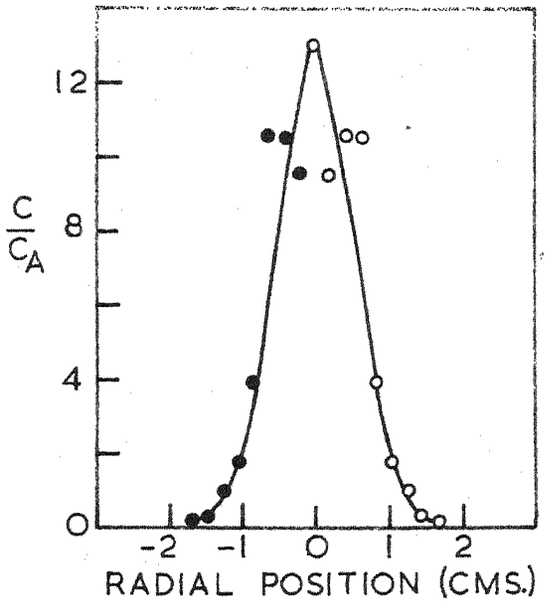

450 GMS BED
Z = 2.475 CM.
F = 7.5 LPM.

FIG 5.13

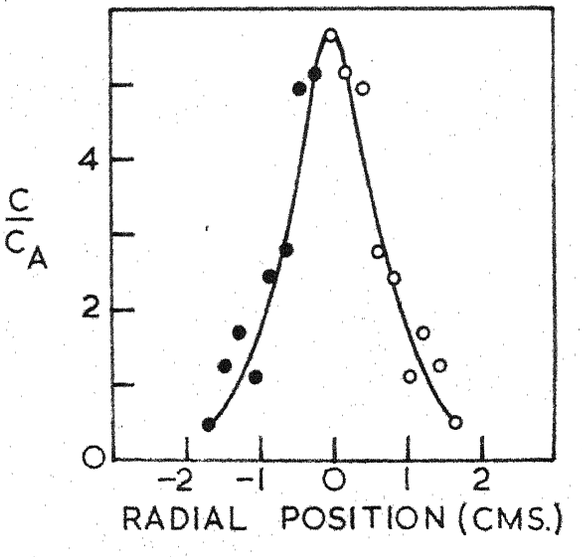

450 GMS BED
Z = 6.285 CM
F = 7.5 LPM

FIG_5.14

TRACER DISTRIBUTION CURVES

● REFLECTED POINTS

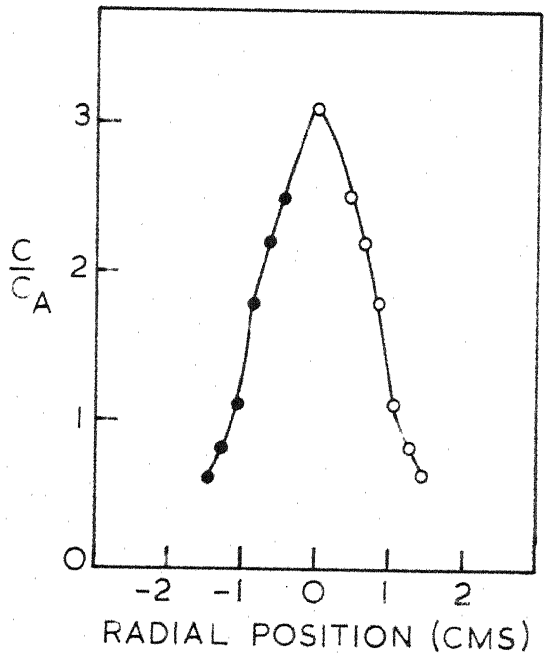

450 GMS BED
Z = 10.095 CM
F = 6 LPM.

FIG_5.15

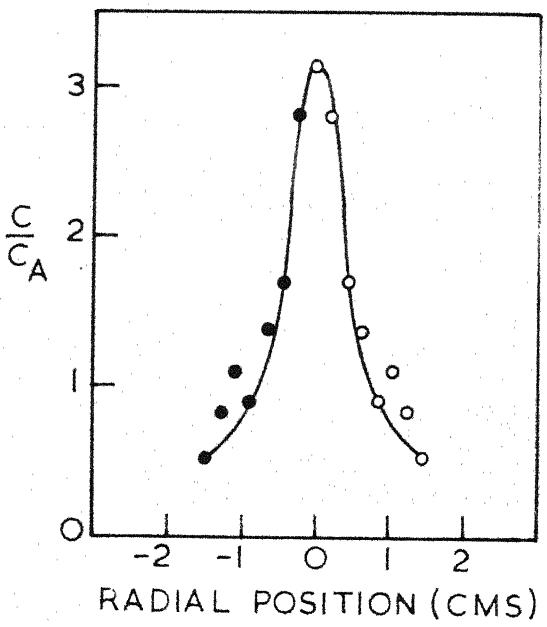

450 GMS BED
Z = 10.095 CM
F = 7 LPM

FIG_5.16

TRACER DISTRIBUTION CURVES

● REFLECTED POINTS

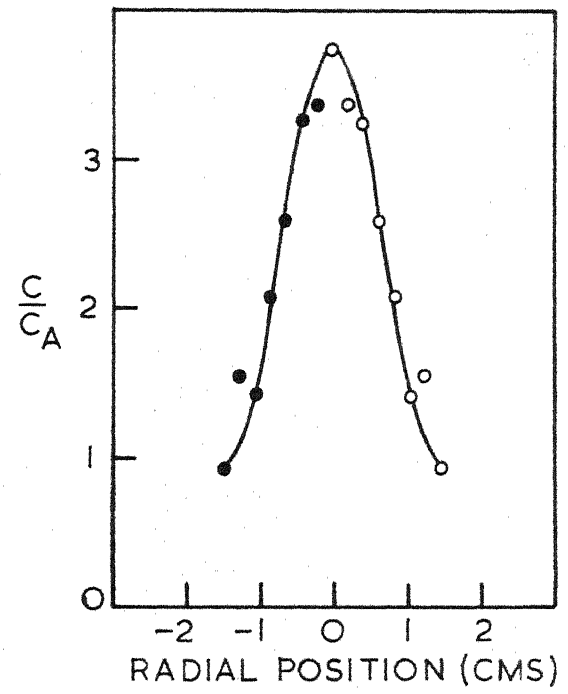

450 GMS BED
Z = 10.095 CM
F = 7.5 LPM

FIG._5.17

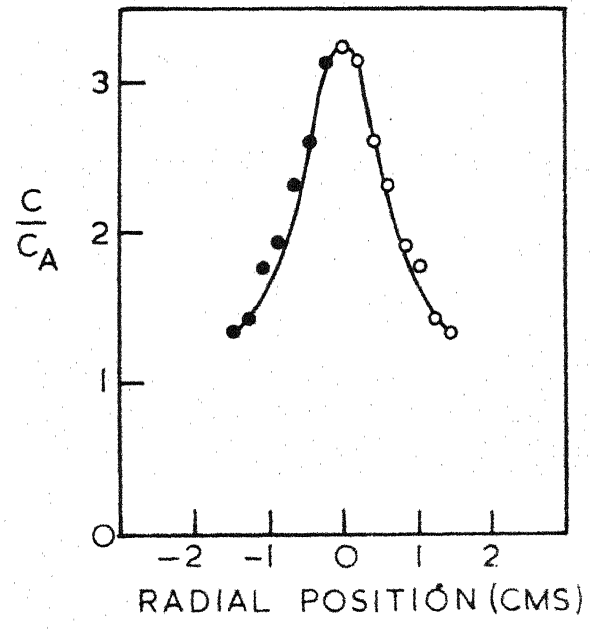

450 GMS BED
Z = 10.095 CM
F = 9 LPM

FIG._5.18

TRACER DISTRIBUTION CURVES

● REFLECTED POINTS

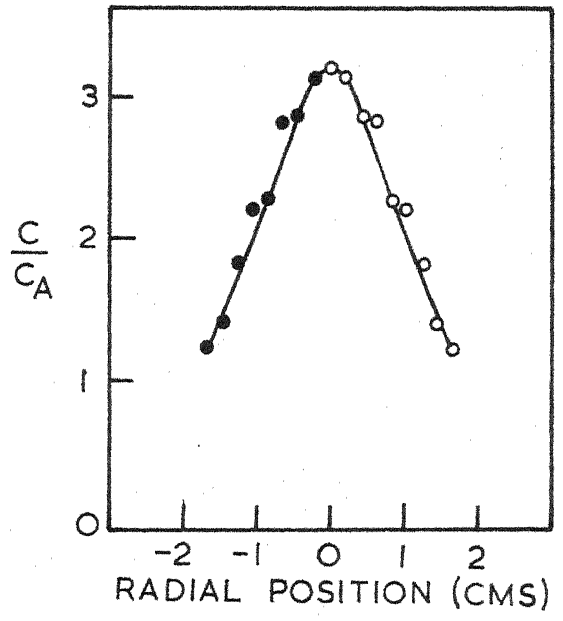

450 GMS BED
Z = 10.095 CM.
F = 10 LPM

FIG._5.19

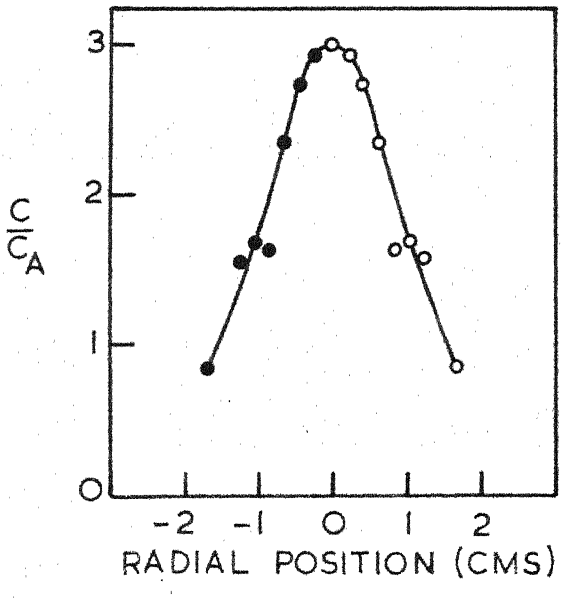

450 GMS BED
Z = 10.095 CM
F = 11 LPM

FIG._5.20

TRACER DISTRIBUTION CURVES

● REFLECTED POINTS

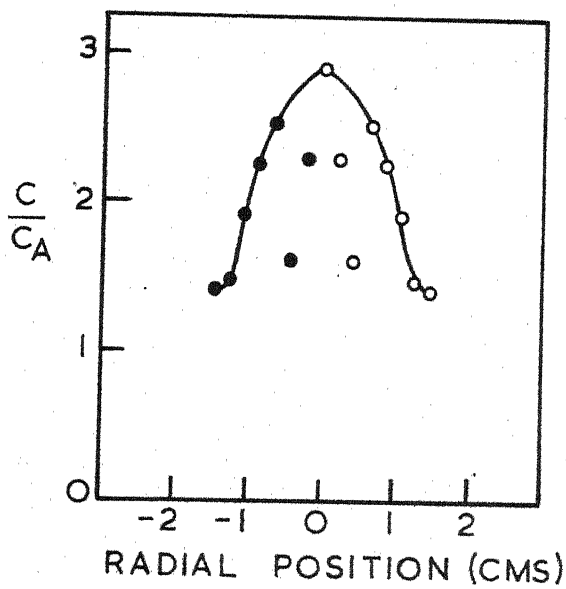

450 GMS BED
Z = 10.095 CM
F = 12 LPM

FIG_5.21

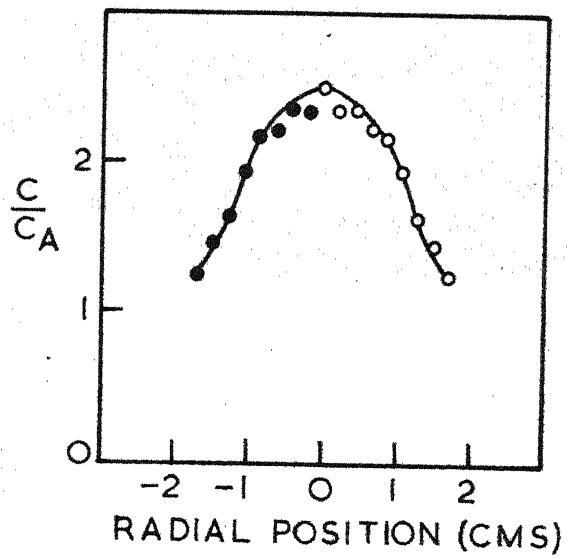

450 GMS BED
Z = 10.095
F = 13 LPM

FIG_5.22

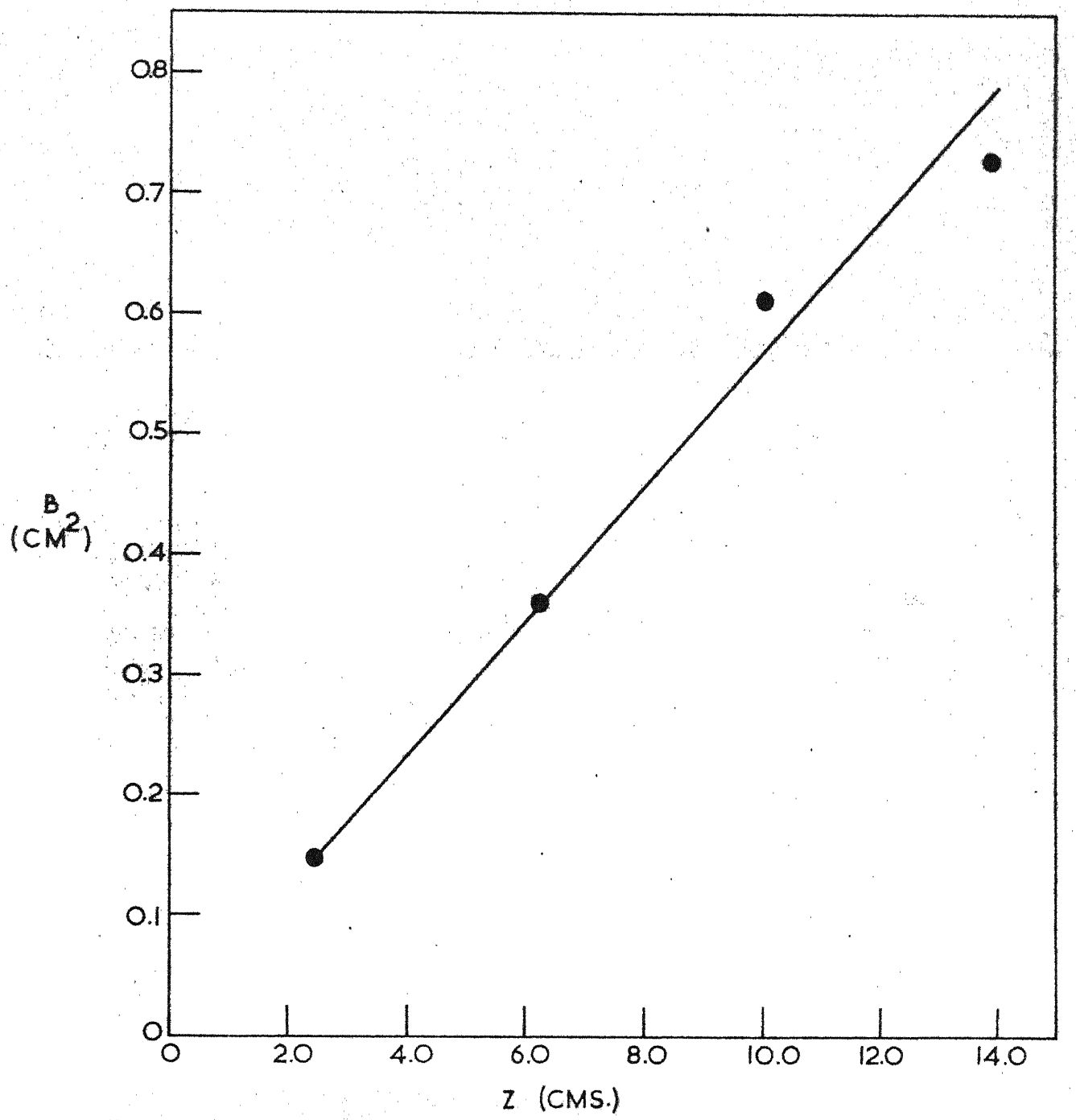

FIG. 5.23_B Vs. Z FOR THE FLUIDIZED BED AT $\epsilon = 0.58$

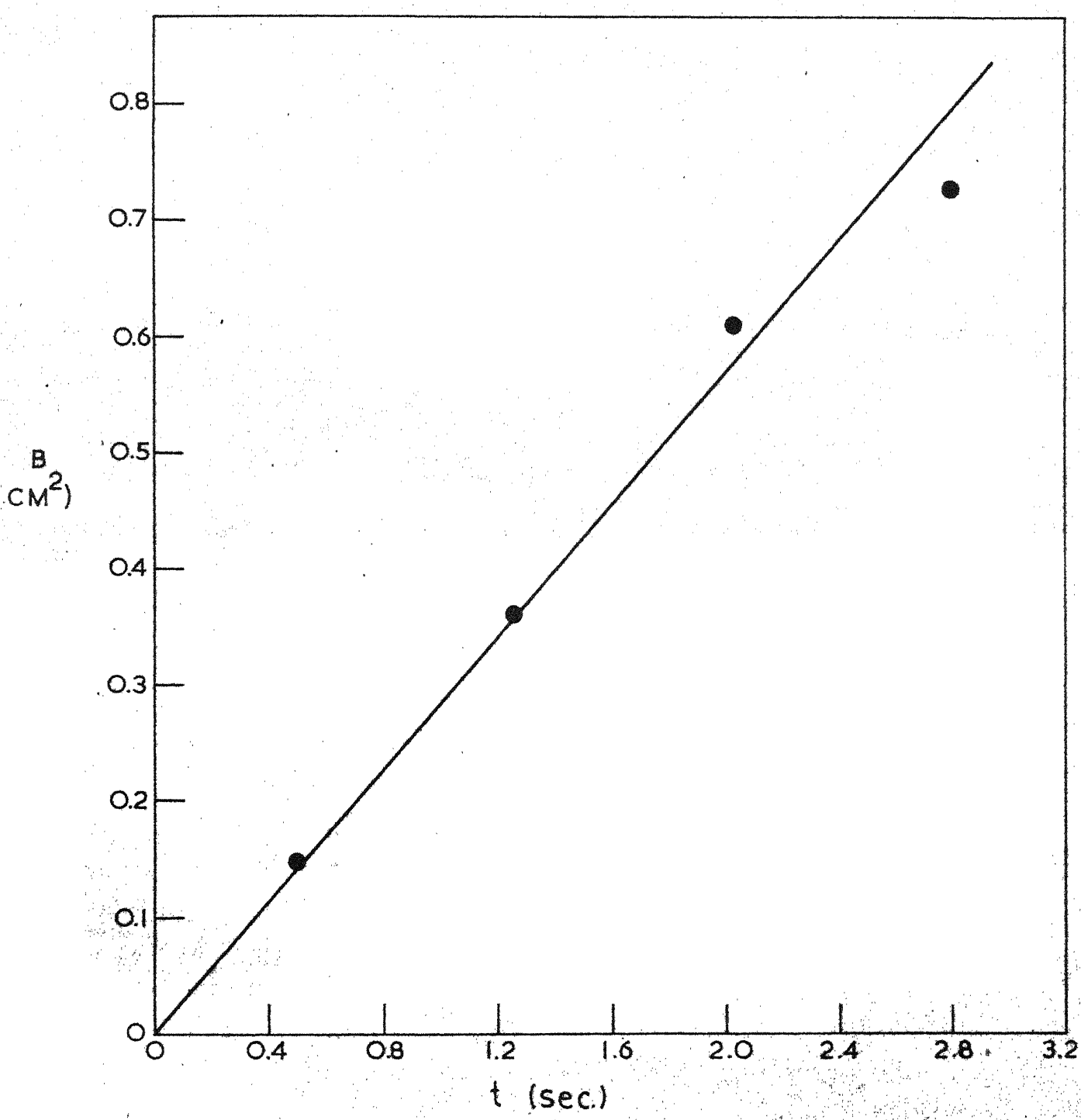

FIG.5.24 'B' Vs. 't' FOR THE FLUIDIZED BED AT $\epsilon = 0.58$ AT DIFFERENT 'Z' POSITIONS

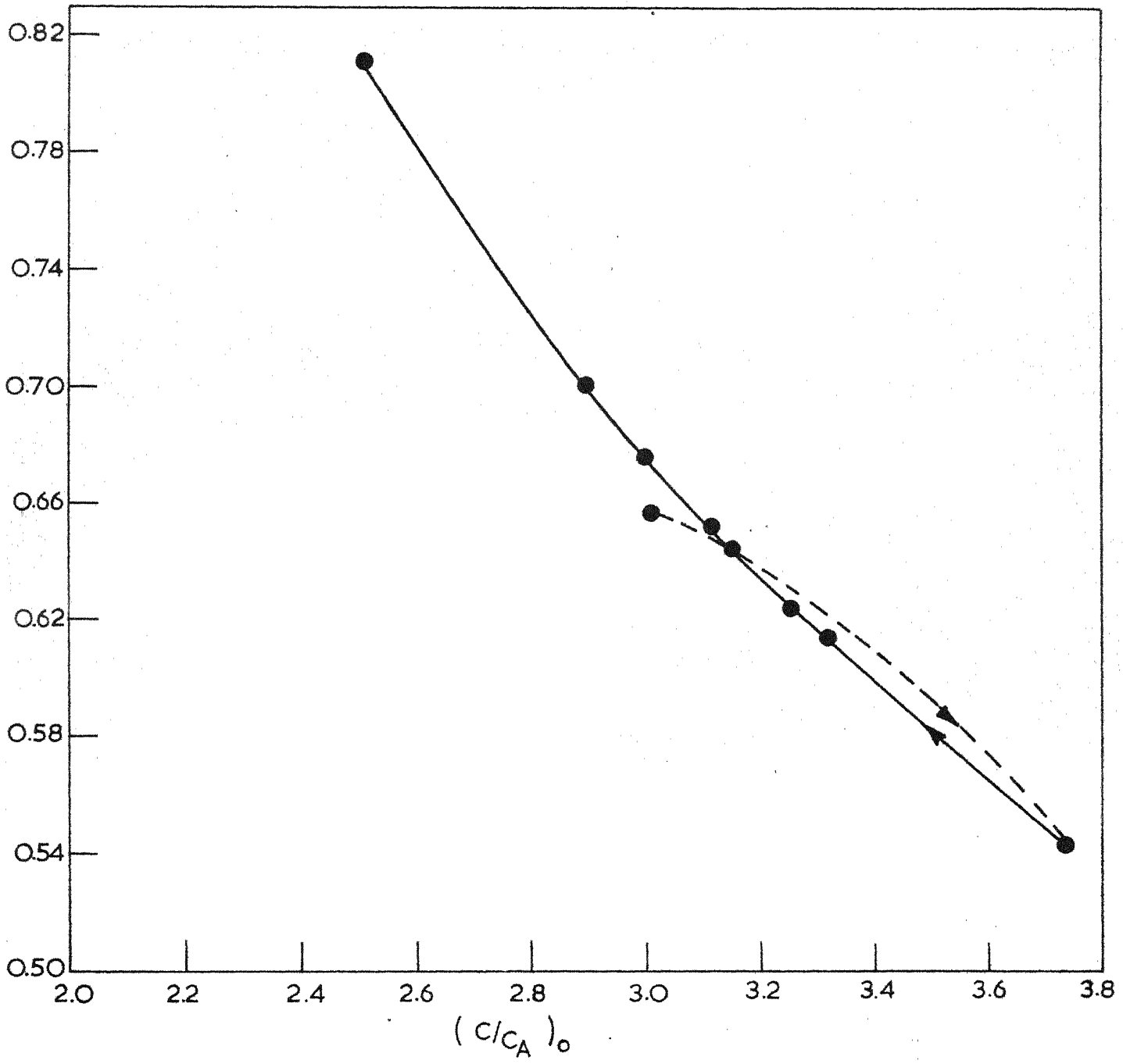

FIG. 5.25_B Vs. CENTER-LINE COMPOSITIONS $(C/C_A)_o$ AT Z = 10.095 CMS. AT DIFFERENT FRACTIONS VOID

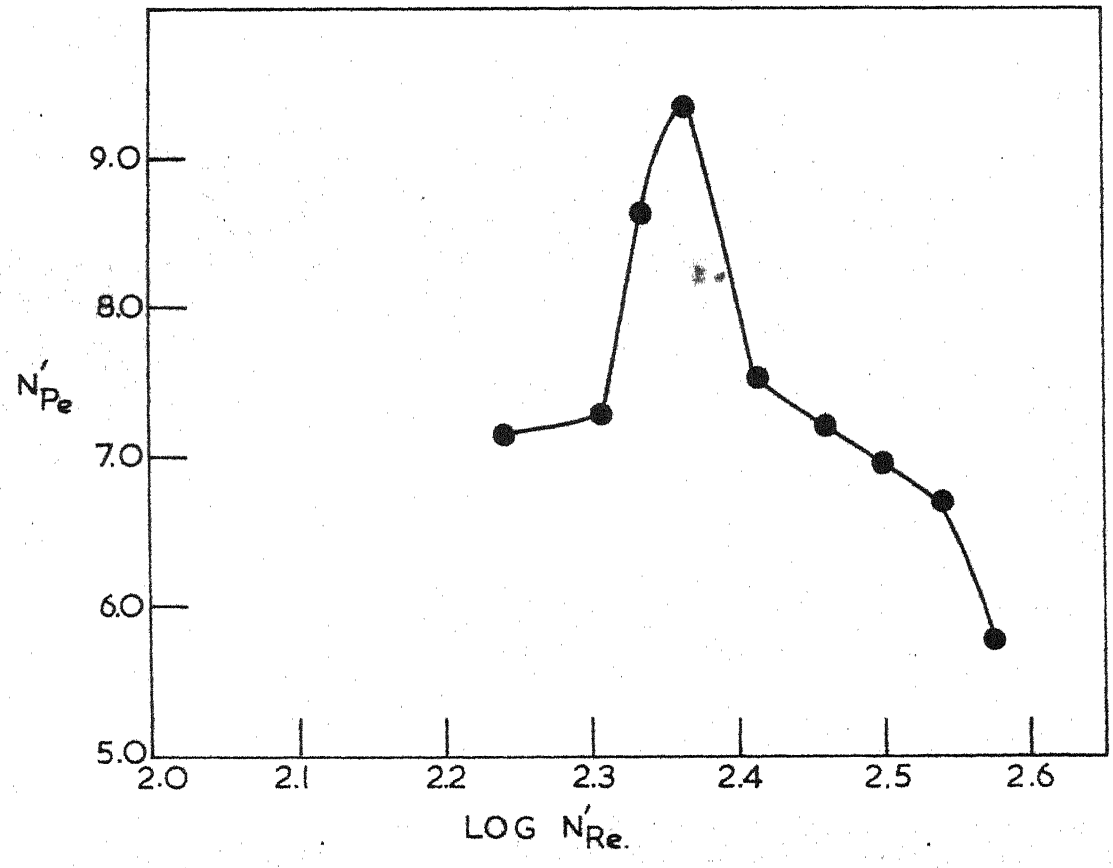

FIG. 5.26 - VARIATION OF PECLET NO. WITH REYNOLDS NO. IN THE BED OF UNIFORMLY SIZED NONSPHERICAL PARTICLES.

REFERENCES

1. Wicke and Trawinski, Chem.Ing.Techn., 1953, 25, No.3, 114-124.
2. Hanratty, Latinen and Wilhelm, A.I.Ch.E. Journ., 1956, 2, 373-380.
3. Blickle and Kaldi, Chem. Techn., 1959, 11, No.4, 181-184.
4. Cairns and Prausnitz, A.I.Ch.E. Journ., 1960, 6, No.3, 400-405.
5. Leva, "Fluidization", 1959.
6. Askins, Hinds and Kunreuther, Chem. Eng. Progr., 1951, 47, 401-404.
7. Gilliland and Mason, Ind. Eng. Chem., 1952, 44, 218-224.
8. Gilliland and Mason, Ind. Eng. Chem., 1953, 45, 1177-1185.
9. Rema, Chem. and Industry, 1955, 15, No.3, 46-51.
10. Handlos, Kungtman and Schissler, Ind. Eng. Chem., 1957, 49, 25-30.
11. Deemter, Chem. Eng. Sci., 1961, 13, No.3, 143-154.

****